Fate plasticity and reprogramming in genetically distinct populations of *Danio* leucophores

Victor M. Lewis[a,b], Lauren M. Saunders[a,c,d], Tracy A. Larson[a], Emily J. Bain[a], Samantha L. Sturiale[a], Dvir Gur[e,f], Sarwat Chowdhury[g,h], Jessica D. Flynn[i], Michael C. Allen[j], Dimitri D. Deheyn[j], Jennifer C. Lee[i], Julian A. Simon[g,h], Jennifer Lippincott-Schwartz[e], David W. Raible[b,k], and David M. Parichy[a,l,1]

[a]Department of Biology, University of Virginia, Charlottesville, VA 22903; [b]Department of Biology, University of Washington, Seattle, WA 98195; [c]Department of Genome Sciences, University of Washington, Seattle, WA 98195; [d]Program in Molecular and Cellular Biology, University of Washington, Seattle, WA 98195; [e]Janelia Research Campus, Howard Hughes Medical Institute, Ashburn, VA 20147; [f]*Eunice Kennedy Shriver* National Institute for Child Health and Human Development, National Institutes of Health, Bethesda, MD 20892; [g]Clinical Research Division, Fred Hutchinson Cancer Research Center, Seattle, WA 98109; [h]Human Biology Division, Fred Hutchinson Cancer Research Center, Seattle, WA 98109; [i]National Heart, Lung, and Blood Institute, National Institutes of Health, Bethesda, MD 20892; [j]Marine Biology Research Division, Scripps Institution of Oceanography, University of California, San Diego, La Jolla, CA 92093; [k]Department of Biological Structure, University of Washington, Seattle, WA 98195; and [l]Department of Cell Biology, University of Virginia, Charlottesville, VA 22903

Edited by Marianne E. Bronner, California Institute of Technology, Pasadena, CA, and approved May 6, 2019 (received for review January 18, 2019)

Understanding genetic and cellular bases of adult form remains a fundamental goal at the intersection of developmental and evolutionary biology. The skin pigment cells of vertebrates, derived from embryonic neural crest, are a useful system for elucidating mechanisms of fate specification, pattern formation, and how particular phenotypes impact organismal behavior and ecology. In a survey of *Danio* fishes, including the zebrafish *Danio rerio*, we identified two populations of white pigment cells—leucophores—one of which arises by transdifferentiation of adult melanophores and another of which develops from a yellow–orange xanthophore or xanthophore-like progenitor. Single-cell transcriptomic, mutational, chemical, and ultrastructural analyses of zebrafish leucophores revealed cell-type–specific chemical compositions, organelle configurations, and genetic requirements. At the organismal level, we identified distinct physiological responses of leucophores during environmental background matching, and we showed that leucophore complement influences behavior. Together, our studies reveal independently arisen pigment cell types and mechanisms of fate acquisition in zebrafish and illustrate how concerted analyses across hierarchical levels can provide insights into phenotypes and their evolution.

pigmentation | neural crest | transdifferentiation | evolution | zebrafish

Vertebrate pigmentation contributes to ecological interactions and is often a target of selection during adaptation and speciation (1–3). Teleost fishes are among the most phenotypically diverse of vertebrate taxa, and their spectacular array of pigment phenotypes support a variety of behaviors, from attracting mates to predator avoidance, social aggregation, and aggressive interactions. In contrast to birds and mammals that have only a single pigment cell type, the melanocyte, teleosts develop multiple pigment cell classes, including black melanophores, yellow–orange xanthophores, and iridescent iridophores. Pigment patterns reflect the relative abundance and spatial locations of these chromatophores. Decades of work have contributed to understanding developmental and genetic bases of black, yellow, and iridescent pigmentation and the cellular interactions underlying pattern formation (4).

Teleosts also develop several additional classes of chromatophores, including white or yellow–white "leucophores" (5). Our knowledge of fate specification, genetic requirements, physical and chemical properties, and behavioral roles of these cells remains fragmentary. Nevertheless, the presumptive origin of all these chromatophores in a common precursor cell population—the embryonic neural crest—and the distinctiveness of these chromatophores in fish that display them suggest an opportunity to dissect phenotypic diversification ranging from genetic mechanisms and cell-fate plasticity to organismal interactions.

Zebrafish *Danio rerio* has emerged as a preeminent laboratory model for studying neural crest development and pigment pattern formation, and comparisons of zebrafish and other *Danio* species have provided insights into the evolution of pattern-forming mechanisms (4, 6–8). Here we investigate physical properties, genetic mechanisms, and cell lineage of leucophores in zebrafish and its relatives. We show that *Danio* fishes have two distinct classes of leucophores with independent developmental origins and cellular architectures. We further identify lineage-specific requirements and pathways modulated in these cells by genetic, chemical, and single-cell transcriptomic analyses, and we show that leucophores potentially impact behaviors at the whole-organism level. Our findings suggest that white pigmentation in *Danio* has resulted from phenotypic convergence in neural crest sublineages, revealing an unexpected mode of pigment cell evolution.

Results

Dual Classes and Origins of Leucophores in *Danio*. We evaluated leucophore distribution across nine species representing multiple subclades within the genus. Leucophores containing orange and white pigment were evident in anal fins of seven species, including zebrafish, and less prominently in dorsal fins of two species (Fig. 1 *A*

Significance

A foundational question in biology is how phenotypically similar traits arise. Here we identify two distinct white pigment cell populations, leucophores, that arise from independent progenitors in zebrafish and its relatives. Remarkably, one of these leucophore populations develops from previously differentiated, black melanophores. These different leucophores exhibited distinct pigment chemistries, cytological features, gene expression profiles, and genetic requirements, and whole-animal experiments implicated these cells in behavioral interactions. Our several approaches provide insights into pigment cell complements and origins in zebrafish and contribute to our understanding of form and function in the spectacular pigment patterns of teleost fishes.

Author contributions: V.M.L., T.A.L., J.D.F., J.L.-S., D.W.R., and D.M.P. designed research; V.M.L., L.M.S., T.A.L., E.J.B., S.L.S., D.G., S.C., and M.C.A. performed research; V.M.L., L.M.S., T.A.L., D.G., S.C., J.D.F., M.C.A., D.D.D., J.C.L., J.A.S., J.L.-S., and D.M.P. analyzed data; and V.M.L., D.W.R., and D.M.P. wrote the paper.

The authors declare no conflict of interest.

This article is a PNAS Direct Submission.

Data deposition: The scRNA-Seq data reported in this paper have been deposited in the National Center for Biotechnology Information Gene Expression Omnibus database, https://www.ncbi.nlm.nih.gov/geo/ (accession no. GSE130526).

[1]To whom correspondence may be addressed. Email: dparichy@virginia.edu.

This article contains supporting information online at www.pnas.org/lookup/suppl/doi:10.1073/pnas.1901021116/-/DCSupplemental.

and *B*, *Left*, and *SI Appendix*, Fig. S1). Similar to xanthophores, these cells contained pteridines and carotenoids (*SI Appendix*, Fig. S2 *A*–*C*). During development, pronounced yellow–orange pigmentation was evident first, with a white halo of pigmentation becoming gradually more distinct over several days (*SI Appendix*, Fig. S2 *D* and *E*). These findings are consistent with some shared characteristics and potentially lineage origins of leucophores and xanthophores, as inferred from visual observations and genetic analyses of medaka fish (9–11). Given the temporal order of pigment deposition in *Danio*, we refer to these cells as "xantholeucophores."

In addition to xantholeucophores, a population of leucophores has been noted in zebrafish as "white cells" at the distal edges of dorsal and caudal fins (12). Across species, eight of nine *Danio* exhibited leucophores lacking orange coloration at the margin of the dorsal fin, in the dorsal and ventral lobes of the caudal fin, and, in two species, within the anal fin (Fig. 1 *A* and *B* and *SI Appendix*, Fig. S1). These cells had reflective but opaque white material that was variably contracted toward the cell body or dispersed in cellular processes (Fig. 1*C*) and lacked pteridines and carotenoids (*SI Appendix*, Fig. S2 *A* and *B*). Because the cells sometimes contained melanin (Fig. 1 *B*, *Right*, and *SI Appendix*, Fig. S1 *B* and *C*) we refer to them as "melanoleucophores."

In zebrafish, melanoleucophores and xantholeucophores expressed distinct pigment cell reporters (Fig. 1*D* and *SI Appendix*, Fig. S3). Melanoleucophores expressed a *tyrosinase related protein 1b* (*tyrp1b*) transgene that marks melanophores, whereas xantholeucophores expressed an *aldehyde oxidase 5* (*aox5*) transgene that marks xanthophores (13). Both melanoleucophores and xantholeucophores expressed a reporter for *purine nucleoside phosphorylase 4a* (*pnp4a*), which is expressed strongly in iridophores and at lower levels in other pigment cells (14, 15)

Whereas xantholeucophores somewhat resembled leucophores of medaka (9), melanoleucophores appeared to be a cell type of unknown origin. We hypothesized that melanoleucophores and melanophores share a lineage, given shared expression of the *tyrp1b* transgene and the sporadic melanin found in melanoleucophores. To test this hypothesis, we labeled cells mosaically (16) using a *mitfa:tdTomato* transgene expressed by pigment cell precursors and melanophores (17). Each of 64 labeled clones containing melanoleucophores also included melanophores, indicating that the cells share a common progenitor or that one cell type transdifferentiates from the other (Fig. 1*E*). To distinguish between these possibilities, we labeled cells with photoconvertible Eos (*pnp4a:nlsEos*) and followed individual cells as they differentiated (13). These analyses demonstrated that melanoleucophores arise directly from melanophores, accumulating white material and losing melanin over several days (Fig. 1*F*). Consistent with this finding, >95% of newly differentiating melanoleucophores, just beginning to acquire white pigment, contained melanin (143 of 150 cells in 10 larvae). Together, these observations indicate that *Danio* develop leucophores of two varieties, with distinct morphologies and origins.

Distinct Requirements for Specification and Morphogenesis. The origins of xantholeucophores from xanthophore-like cells, and melanoleucophores from melanophores, suggested that their development would involve genes required for these respective lineages. Colony-stimulating

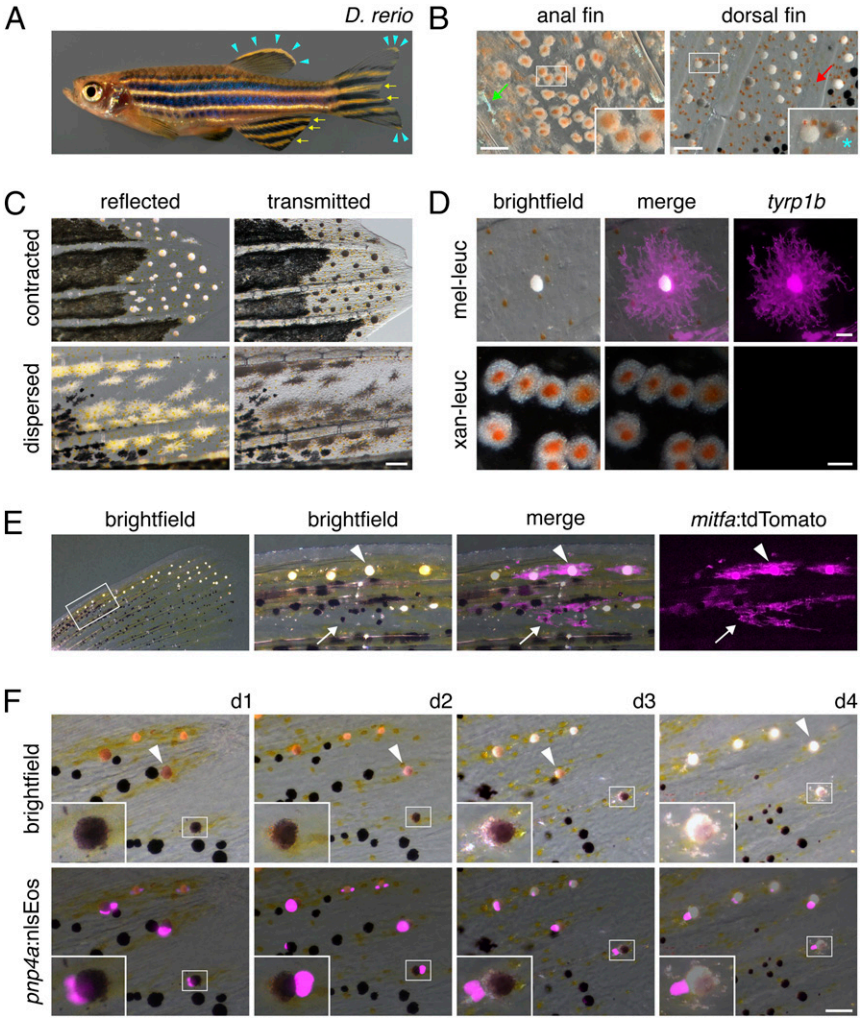

Fig. 1. Leucophore appearance and origins in zebrafish. (*A*) Pigment cells containing white pigment. Arrows, leucophores containing yellow–orange pigment. Arrowheads, white cells lacking orange pigment. (*B*, *Left*) Leucophores with white and orange pigment. (*B*, *Right*) Cells containing white pigment. (*B*, *Insets*) Higher magnification, including gray melanin-containing cell (asterisk). Green arrow, iridescent iridophore. Red arrow, orange pigment of xanthophore. Fish were treated with epinephrine to contract pigment granules. (*C*) Leucophores at tips of caudal fins under reflected and transmitted illumination. (*D*) Melanoleucophores but not xantholeucophores expressed *tyrp1b*:palm-mCherry. (*E*) Labeled clones contained melanoleucophores (arrowhead) and melanophores (arrow). (*F*) Acquisition of white pigment by a melanophore over 4 d (boxed cell; *Inset*). Arrowhead, a second cell that transits distally. (Scale bars: *B*, 50 μm; *C*, 100 μm; *D*, *Upper*, 20 μm and *Lower*, 10 μm; *E* and *F*, 40 μm.)

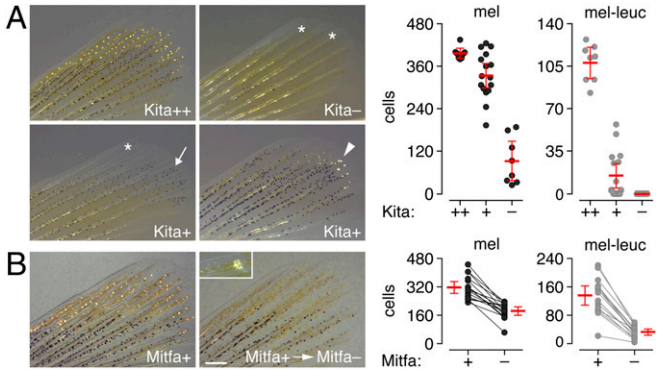

Fig. 2. Distinct requirements for Kita and Mitfa. (*A*) *kita*^{j1e99} at permissive temperature (Kita++) had wild-type complements of melanophores and melanoleucophores, but at restrictive temperature (Kita–) were deficient for melanophores and lacked all melanoleucophores (asterisks). At intermediate temperature (Kita+), melanophores were abundant but locations normally harboring melanoleucophores were devoid of these cells (asterisk, *Left*), populated by melanophores (arrow, *Left*), or had fewer melanoleucophores compared with permissive temperature (arrowhead, *Right*). Plots, cell numbers for individual fish ($F_{2,29}$ = 65.2 and 119.2, respectively, $P < 0.0001$; bars, means ± 95% CI). (*B*) *mitfa*^{vc7} fish at permissive temperature (Mitfa+) developed melanophores and melanoleucophores, but many of each died on transition to restrictive temperature (Mitfa–). Panels show same fish before and 2 d after transition. (*B*, *Inset*) White pigment containing cellular debris indicative of cell death [e.g., ref. 50]. Plots, cell numbers for individual fish before and after transition (paired t_{15}= −8.6 and −10.9, respectively, $P < 0.0001$; bars, means ± 95% CI). Controls maintained at permissive temperature exhibited 1% increases in numbers of each cell type over this period (paired $t_{15} = 3.2$, $P < 0.05$ and paired $t_{15} = 2.2$, $P = 0.06$, respectively). (Scale bar: 250 μm).

factor-1 receptor-a (Csf1ra) and Kit-a (Kita) promote the development of xanthophores and melanophores, respectively (18, 19). Consistent with our expectation, *csf1ra* mutants lacked xantholeucophores but retained melanoleucophores, and *kita* mutants lacked melanoleucophores but retained xantholeucophores (*SI Appendix*, Figs. S4 *A*, *B*, and *D*). Thus, different types of leucophores have different genetic requirements. Leukocyte tyrosine kinase (Ltk) is required by iridophores but not xanthophores or melanophores (20), and *ltk* mutants retained both leucophore classes (*SI Appendix*, Fig. S4*A*).

We further asked if melanoleucophores have distinct requirements for pathways essential to melanophore development. Because different levels of Kit signaling can promote different cellular outcomes (21, 22), we speculated that melanoleucophores and melanophores might have different requirements for Kita activity. We therefore compared phenotypes of the temperature-sensitive allele *kita*^{j1e99} at permissive, restrictive, and intermediate temperatures (23). At permissive temperature, normal complements of both cell types were present; at restrictive temperature, both cell types were missing (Fig. 2*A*). At intermediate temperature, 91% of melanophores but only 14% of melanoleucophores developed (Fig. 2*A*). These findings, and the presence of melanophores in regions normally occupied by melanoleucophores, support a model in which melanoleucophore differentiation requires more Kita signaling than melanophore development or maintenance.

The Melanocyte-inducing transcription factor (Mitf) is necessary for fate specification, melanogenesis, and survival of melanocytes in mammals, and its homolog, Mitfa, has conserved roles in melanophores (24, 25). Mutants for *mitfa* lacked melanophores and melanoleucophores (*SI Appendix*, Fig. S4*C*). To test if differentiated melanoleucophores themselves require Mitfa or if their deficit results only from a lack of their melanophore progenitors, we employed the temperature-sensitive allele *mitfa*^{vc7} (26, 27). We reared fish at permissive temperature to allow melanophore and melanoleucophore differentiation and then shifted the fish to restrictive temperature to curtail Mitfa availability. This condition resulted in the loss of 42% of melanophores and 76% of melanoleucophores within 2 d (Fig. 2*B*). Thus, Mitfa is necessary for survival of differentiated melanoleucophores in addition to development of their melanophore progenitors.

Distinct Organelle Ultrastructures and Chemistry of Melanoleucophore and Xantholeucophore White Coloration. To address physical and chemical bases for white coloration, we examined spectral properties of leucophores. Both melanoleucophores and xantholeucophores reflected across a wide spectrum (*SI Appendix*, Fig. S5*A*). Moreover, both cell types lacked the angular-dependent change of hues—iridescence—of iridophores, which results from stacked arrangements of crystalline guanine reflecting platelets within membrane-bound organelles (5, 28, 29) (Fig. 3*A*). Accordingly, we predicted and then observed by transmission electron microscopy (TEM) that both cell types lack ordered reflecting platelets. Melanoleucophores exhibited variably shaped organelles distinct from reflecting platelets and melanosomes (Fig. 3 *B* and *C*). Xantholeucophores were similar to leucophores of other species and xanthophores of zebrafish (*SI Appendix*, *Materials and Methods*, *TEM*) in harboring round organelles—carotenoid vesicles containing yellow–orange pigment—as well as irregular organelles indistinguishable from pterinosomes, which contain yellow or colorless pteridines (Fig. 3*D* and *SI Appendix*, Fig. S5*B*).

We used mass spectrometry to assay purine contents of fin tissue containing different pigment cell classes. Guanine but not other purines was detected in excess in tissues specifically containing melanoleucophores (Fig. 3*E* and *SI Appendix*, Fig. S5 *C* and *D*). Raman spectroscopy of individual melanoleucophores revealed crystalline β-guanine, the metastable phase of guanine, typical of iridophores and other biological systems in which crystallization is

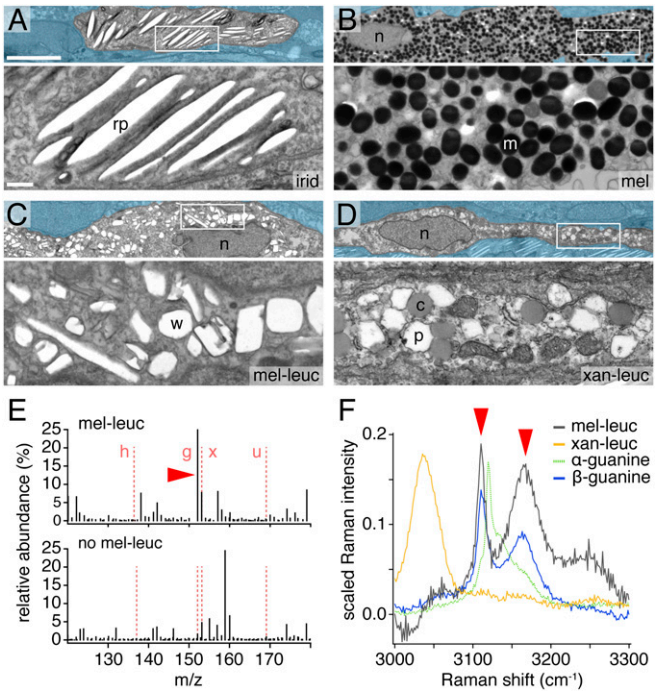

Fig. 3. Ultrastructural and chemical characteristics of melanoleucophores and xantholeucophores. (*A–D*) Fin iridophores (*A*) exhibited reflecting platelets (rp) and melanophores had typical melanosomes (m). Melanoleucophores (*C*) contained irregularly shaped and arranged organelles (w) presumptively containing white material, whereas xantholeucophores (*D*) contained presumptive pterinosomes (p) and carotenoid vesicles (c), without other organelles likely to harbor white pigment. (*Upper*) Low magnification with adjacent cells masked. (*Lower*) Boxed regions. n, nucleus. (*E*) Mass spectrometry of fin tissue containing melanoleucophores (*Upper*) revealed more abundant guanine (arrowhead) compared with fin tissue without melanoleucophores (*Lower*; h, hypoxanthine; g, guanine; x, xanthine; u, uric acid). (*F*) Representative Raman spectra of melanoleucophores (gray; $n = 19$ cells) and xantholeucophores (orange; $n = 14$) compared with α-guanine and β-guanine. High energy peak pattern (arrowheads) indicates β-guanine is present in melanoleucophores but is not detectable in xantholeucophores. (Scale bars: *Upper* 5 μm, *Lower* 500 nm).

regulated (30, 31) (Fig. 3*F*). Tissue harboring xantholeucophores had somewhat increased guanine content (*SI Appendix*, Fig. S5*E*) although crystalline forms of guanine were not detectable (Fig. 3*F*). This suggests that other factors contribute to white pigmentation in these cells. Together, these analyses indicate distinct ultrastructural and chemical bases for white pigmentation of melanoleucophores and xantholeucophores.

Melanoleucophores and Xantholeucophores Differentially Modulate Pigment Synthesis Pathways. We hypothesized that differentiation of melanoleucophores from melanophores would involve a switch from melanin to purine synthesis and therefore analyzed transcriptomes of individual pigment cells during melanoleucophore development. Dimensionality reduction and clustering followed by empirical validation of cluster assignments identified melanophores and melanoleucophores, as well as xanthophores and xantholeucophores (Fig. 4 *A* and *B* and *SI Appendix*, Fig. S6). Supporting a developmental switch in pigmentation pathways, melanoleucophores exhibited higher expression of genes for de novo purine synthesis, but lower expression of genes for melanin synthesis, compared with melanophores (Fig. 4 *C* and *D*). Pseudotemporal ordering of cells (32) along a differentiation trajectory (Fig. 4 *B*, *Right*) likewise revealed an inverse relationship in gene expression between purine and melanin synthesis pathways (Fig. 4 *E* and *F*). This sequence raised the possibility that acquisition of white pigment might depend on prior melanization; that mutants with unmelanized melanophores develop melanoleucophores allowed us to reject this model (*SI Appendix*, Fig. S7*A*).

Compared with melanoleucophores and melanophores, xantholeucophores and xanthophores occupied more distinct locations in transcriptomic space (Fig. 5 *B*, *Left*) (33). A differentiation trajectory likewise revealed few cells of intermediate states (*SI Appendix*, Fig. S7*B*), suggesting that differentiating xantholeucophores were not well represented and that xanthophores (from dorsal fin) were an inadequate proxy for early states of xantholeucophore differentiation. Genes involved in purine synthesis, carotenoid processing, and pteridine synthesis were all expressed at higher levels in xantholeucophores than in nonpigment cells (*SI Appendix*, Fig. S7 *C* and *D*).

Physiological Responses and Behavioral Implications of *Danio* Leucophores. We sought to understand how leucophores might impact phenotype at the organismal level. During ambient background color adaptation, zebrafish and other species physiologically contract or disperse pigment-containing organelles within pigment cells. Typically, melanosomes of melanophores are contracted on a light background, yielding a lighter fish, but are dispersed on a dark background, yielding a darker fish. Leucophores of medaka and *Fundulus* have the opposite response of melanophores (34–36). Given the distinct properties of melanoleucophores and xantholeucophores in *Danio*, we predicted that they would have different physiological responses as well. Under standard conditions, guanine deposits of *Danio* melanoleucophores were often contracted whereas pigment deposits of xantholeucophores were often expanded (*SI Appendix*, Fig. S1 *B*, *Top*). Melanoleucophores responded, as did melanophores, by contracting pigment organelles centripetally in the light and dispersing them peripherally in the dark (Fig. 5 *A* and *B*). Xantholeucophores displayed the opposite response. Thus, melanoleucophores and xantholeucophores have opposing physiological responses during background adaptation.

Finally, we asked whether social behavior might be influenced by melanoleucophores, given their prominent position on the fins, which are held erect during aggressive and courtship interactions (37). To test if zebrafish can perceive and respond to tissue containing melanoleucophores, we presented fish with alternative shoals having intact melanoleucophores (sham-manipulated) or excised melanoleucophores (*SI Appendix*, Fig. S8 *A* and *B*). Overall, test fish spent significantly more time in proximity to shoals having intact melanoleucophores (Fig. 5*C*). The first approach of test fish to stimulus shoals also varied with melanoleucophore status (*SI Appendix*, Fig. S8*C*). These differences are consistent with a model in which fish attend to the presence of melanoleucophores and raise

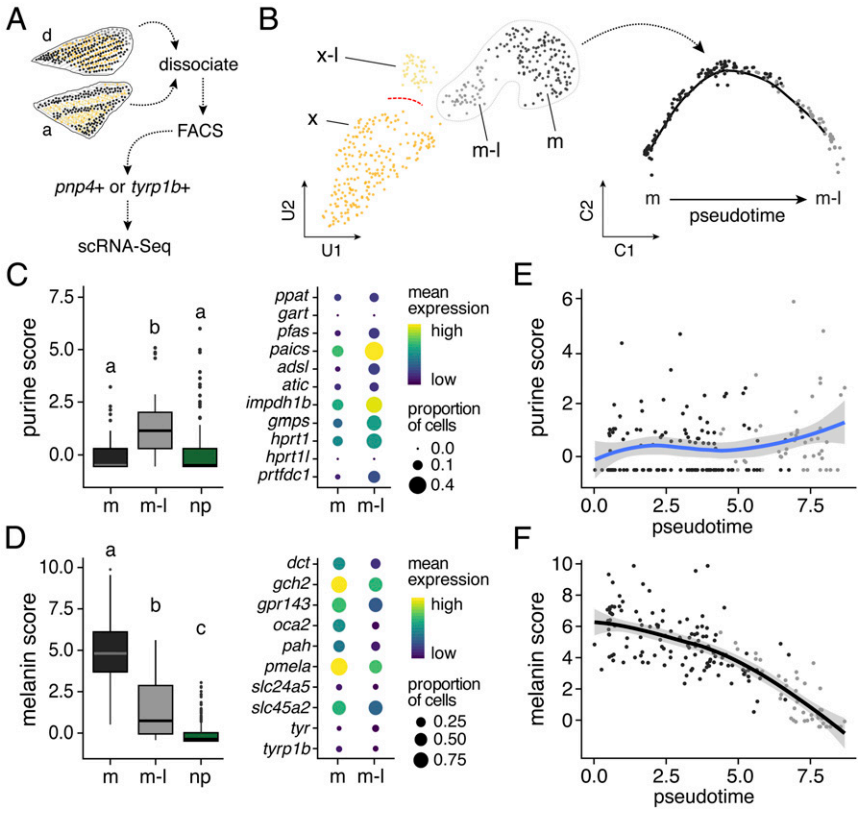

Fig. 4. Pigmentation pathway switch during melanoleucophore maturation. (*A*) Experimental design. d, dorsal fin. a, anal fin. (*B*) 2D UMAP representation (*SI Appendix, Materials and Methods*) of pigment cell clusters (*Left*; x, xanthophores; x-l, xantholeucophores; m, melanophores; m-l, melanoleucophores) and differentiation trajectory (*Right*) of melanophores to melanoleucophores. Red dotted line, cell-free space. (*C*) Aggregate score for de novo purine synthesis genes was greater in melanoleucophores than melanophores or nonpigment cells (np). Box plots, medians with interquartile ranges; different letters indicate differences significant in post hoc comparison ($P < 0.0001$; shared letters, $P = 0.2$). Bubble plots show individual gene expression. (*D*) Melanin synthesis gene expression was reduced in melanoleucophores compared with melanophores. (*E* and *F*) Purine and melanin synthesis gene expression scores for individual cells arranged in pseudotime (arbitrary scale) from melanophore (*Left*) to melanoleucophore (*Right*). Line and shaded region, smoothed average with 95% CI.

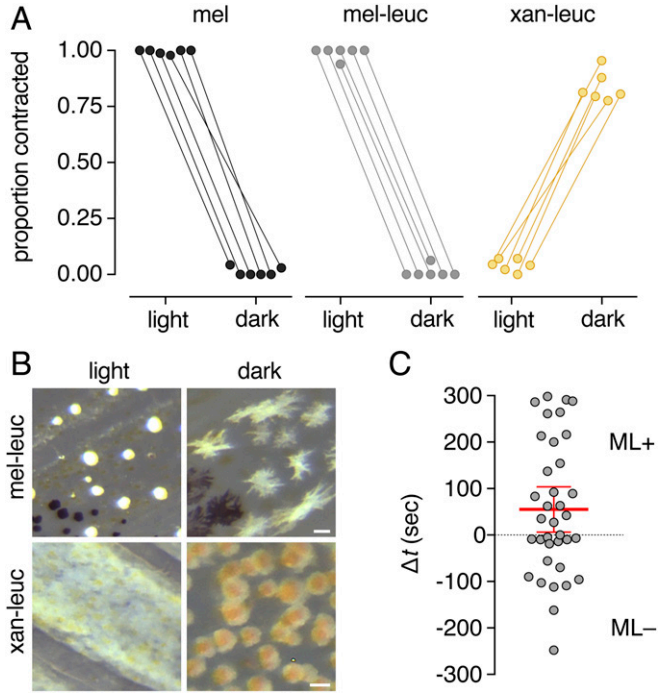

Fig. 5. Background adaptation and behavioral responses. (*A* and *B*) Melanophores and melanoleucophores exhibited the same background adaptation responses whereas xantholeucophores had opposite responses. Points connected by line indicate cells of a single fish ($n = 26$–133 cells, median = 62 cells). (*C*) Whole-fish behavioral response to stimulus fish with intact melanoleucophores (sham-manipulated, ML+) or excised melanoleucophores (ML–). If test fish cannot perceive a phenotypic difference between shoals, or do not respond to it, they should spend equal times with each stimulus type (difference in time spent, $\Delta t = t_{intact} - t_{ablated} = 0$). If test fish perceive and respond to a phenotypic difference, they should spend more time in association with one shoal than the other ($\Delta t \neq 0$). Longer times spent on average with ML+ over ML– shoals indicated a preference for fish retaining melanoleucophore-containing fin tissue (red bars, means ± 95% CI; $\Delta t = 55.0 \pm 48.7$ s; null hypothesis $\Delta t = 0$, two-tailed $t_{35} = 2.29$, $P = 0.03$). Times did not differ with sex of test fish, sex of stimulus fish, or their interaction (ANOVA, all $P \geq 0.18$). (Scale bars: 20 μm).

the possibility of these cells contributing to social interactions in the wild.

Discussion

Our observations that melanoleucophores transdifferentiate from melanophores while xantholeucophores arise from cells resembling xanthophores suggest that a *Danio* ancestor evolved two types of leucophores independently (*SI Appendix*, Fig. S9*A*). These findings, in conjunction with an iridophore requirement for white bars of the clownfish *Amphiprion* (38), suggest that each of the three major chromatophore lineages can contribute to a white pigmentary phenotype.

An unresolved question in the evolution of morphology is the extent to which similar but independently evolved phenotypes depend on the same (parallel) or different (convergent) mechanisms. In melanoleucophores, the deposition of guanine crystals suggests a co-option of purine synthesis and biomineralization mechanisms similar to those of iridophores. However, melanoleucophore crystals are displayed in organelles having morphologies and arrangements differing from those of iridescent and noniridescent (white) iridophores, revealing parallelism in pigmentary composition (guanine crystals) but convergence in cellular architectures to generate a white phenotype (*SI Appendix*, Fig. S9*A*). Melanoleucophores of *Danio* and leucophores of medaka also seem to have arrived independently at a white phenotype through convergence in cell lineage (melanophore vs. shared progenitor with xanthophores or erythrophore), pigmentary composition (guanine vs. uric acid), and ultrastructure (10, 11, 39).

By contrast, our analyses of *Danio* xantholeucophores, which might be expected to resemble medaka leucophores, failed to reveal substantial deposition of either guanine or uric acid, suggesting that these cells have converged on a means of generating a white phenotype that differs from both melanoleucophores and noniridescent iridophores. White material in xantholeucophores might be pteridines (39, 40), given their abundance in these cells. A definitive characterization, and determination of potential roles for small amounts of purines, will require additional analyses.

Beyond evolutionary considerations, this study provides insights into plasticity in cell fate. Over 60 y ago it was observed that amphibian xanthophores can transform into melanophores in the context of interspecies transplantation (41). Likewise, dedifferentiation followed by redifferentiation occurs during regeneration and can be induced experimentally (42–44). Whether cells convert from one differentiated state to another—i.e., transdifferentiate—during normal development has been less clear. Our demonstration that melanoleucophores develop directly from melanophores identifies a natural example of transdifferentiation, corroborating hints that cell states are not as definitive as once thought (45) and highlighting the potential of teleost chromatophores for understanding cell-state dynamics.

The mechanisms responsible for melanoleucophore and xantholeucophore fate specification are not yet known. Nevertheless, our findings do reveal some functions of known pigmentary genes during the development of these cells. The dependence of xantholeucophores and melanoleucophores on xanthogenic *csf1ra* and melanogenic *kita*, respectively, supports a model in which leucophore deployment is constrained by prior lineage requirements (*SI Appendix*, Fig. S9*A*). Our analysis also uncovered a role for *mitfa* in xantholeucophore development, and conditional genetic analyses indicate roles for *kita* and *mitfa* in melanoleucophores, independent of roles in melanophores. It remains for future studies to interrogate how these and other "classic" pigmentation genes integrate with pathways required for the white pigmentary phenotype—including up-regulation of de novo purine synthesis, down-regulation of melanin synthesis, and factors underlying melanin depletion. An intriguing possibility is that *mitfa* itself plays a role, analogous to functions in fate specification or phenotype switching in melanocytes, melanophores, and melanoma (46).

Finally, white pigmentation is thought to be ecologically relevant: white bars of clownfish contribute to species recognition (47), a yellow–white bar in the caudal fin of male Goodeinae fishes is linked to mating success (48), and white pigmentation in fins of the guppy *Poecilia reticulata* likely enhances honest signaling in sexual selection (49). In our study, melanoleucophores and xantholeucophores responded physiologically during background adaptation, suggesting consequences for the avoidance of predation. Moreover, individual fish preferred to associate with stimulus shoals having intact melanoleucophores and differentially approached these shoals depending on sex and melanoleucophore complement. These observations, the prominent position of melanoleucophores, and their likely visibility in habitats experienced by zebrafish (6) all raise the possibility that *Danio* leucophores contribute to social interactions in the wild. In this regard, differences in fin-specific complements of these cells among *Danio* species may be especially interesting.

Materials and Methods

Fish Rearing, Lineage Analysis, and Temperature-Shift Experiments. Zebrafish and other *Danio* species were housed at ~28 °C, 14 h light:10 h dark and fed rotifers, *Artemia*, and flake food. Clonal labeling and Eos-fate mapping followed (13, 16). Fish were anesthetized in MS222 before imaging or fin clipping. Protocols were approved by Institutional Animal Care and Use Committees of the University of Virginia and University of Washington.

Physical and Chemical Analyses. Measurement of reflectance and transmittance used a PARISS hyperspectral imaging system mounted on a Nikon Eclipse 80i microscope. TEM used standard methods. Guanine content was analyzed on an Agilent HPLC with photodiode array detector and single quadrupole mass spectrometer after extracting purines in 1 M NaOH and also using a custom-built Raman microscope.

Single-Cell RNA-Sequencing and Analysis. Cells expressing *tyrp1b*:palm-mCherry or *pnp4a*:palm-mCherry were isolated by fluorescence-activated cell sorting, captured in a Chromium controller (10X Genomics), and sequenced on an Illumina NextSeq 500. Visualization used UMAP (33) with clusters validated using cells of specific phenotypes collected manually and tested by RT-PCR. Trajectory analysis used Monocle (v2.99.1). Gene sets for signature scores were manually curated from the literature and ZFIN: The Zebrafish Information Network.

Physiological and Behavioral Response Testing. Fish were tested for background adaptation in black or white beakers under constant light for 5 min. Behavioral assays were tested for the effects of sham manipulation or melanoleucophore excision as well as for the sex of both test and stimulus fish.

ACKNOWLEDGMENTS. We thank J. Liu for observations and discussions related to xantholeucophores, A. Schwindling and D. White for assistance with fish rearing, A. Wills for microscope use, and E. Parker for assistance with TEM. We additionally note our appreciation of Stephen L. Johnson (deceased), who first documented white cells in zebrafish and who made fundamental contributions to both zebrafish pigmentation research and genetics, including the isolation and use of temperature-sensitive alleles employed in this study. This work was supported by NIH Grant R35 GM122471 (to D.M.P.); National Eye Institute Grant P30 EY001730 Core Grant for Vision Research to the University of Washington Department of Ophthalmology Vision Core; Multidisciplinary University Research Initiative-Melanin Grant AFOSRT FA9550-18-1-0142 (to D.D.D.); and Human Frontiers Cross-Disciplinary Postdoctoral Fellowship LT000767/2018 (to D.G.). J.D.F. and J.C.L. were supported by the Intramural Research Program of the NIH, National Heart, Lung, and Blood Institute.

1. A. C. Price, C. J. Weadick, J. Shim, F. H. Rodd, Pigments, patterns, and fish behavior. *Zebrafish* **5**, 297–307 (2008).
2. J. K. Hubbard, J. A. Uy, M. E. Hauber, H. E. Hoekstra, R. J. Safran, Vertebrate pigmentation: From underlying genes to adaptive function. *Trends Genet.* **26**, 231–239 (2010).
3. N. J. Marshall, F. Cortesi, F. de Busserolles, U. E. Siebeck, K. L. Cheney, Colours and colour vision in reef fishes: Past, present and future research directions. *J. Fish Biol.* 10.1111/jfb.13849 (2018).
4. L. B. Patterson, D. M. Parichy, Zebrafish pigment pattern formation: Insights into the development and evolution of adult form. *Annu. Rev. Genet.* 10.1146/annurev-genet-112618-043741 (2019).
5. M. Schartl *et al*., What is a vertebrate pigment cell? *Pigment Cell Melanoma Res.* **29**, 8–14 (2016).
6. D. M. Parichy, Advancing biology through a deeper understanding of zebrafish ecology and evolution. *eLife* **4**, e05635 (2015).
7. L. B. Patterson, E. J. Bain, D. M. Parichy, Pigment cell interactions and differential xanthophore recruitment underlying zebrafish stripe reiteration and Danio pattern evolution. *Nat. Commun.* **5**, 5299 (2014).
8. J. E. Spiewak *et al*., Evolution of Endothelin signaling and diversification of adult pigment pattern in Danio fishes. *PLoS Genet.* **14**, e1007538 (2018).
9. T. Kimura *et al*., Leucophores are similar to xanthophores in their specification and differentiation processes in medaka. *Proc. Natl. Acad. Sci. U.S.A.* **111**, 7343–7348 (2014).
10. Y. Nagao *et al*., Sox5 functions as a fate switch in medaka pigment cell development. *PLoS Genet.* **10**, e1004246 (2014).
11. T. Hama, "Chromatophores and iridocytes" in *Medaka (Killifish) Biology and Strains*, T. Yamamoto, Ed. (Keigaku Publishing Co., Tokyo,1975), pp. 138–153.
12. S. L. Johnson, D. Africa, C. Walker, J. A. Weston, Genetic control of adult pigment stripe development in zebrafish. *Dev. Biol.* **167**, 27–33 (1995).
13. S. K. McMenamin *et al*., Thyroid hormone-dependent adult pigment cell lineage and pattern in zebrafish. *Science* **345**, 1358–1361 (2014).
14. K. Petratou *et al*., A systems biology approach uncovers the core gene regulatory network governing iridophore fate choice from the neural crest. *PLoS Genet.* **14**, e1007402 (2018).
15. Saunders LM, *et al*., Thyroid hormone regulates distinct paths to maturation in pigment cell lineages. *bioRxiv*, 10.1101/527341 (2019).
16. S. Tu, S. L. Johnson, Fate restriction in the growing and regenerating zebrafish fin. *Dev. Cell* **20**, 725–732 (2011).
17. K. Curran, D. W. Raible, J. A. Lister, Foxd3 controls melanophore specification in the zebrafish neural crest by regulation of Mitf. *Dev. Biol.* **332**, 408–417 (2009).
18. D. M. Parichy, J. F. Rawls, S. J. Pratt, T. T. Whitfield, S. L. Johnson, Zebrafish sparse corresponds to an orthologue of c-kit and is required for the morphogenesis of a subpopulation of melanocytes, but is not essential for hematopoiesis or primordial germ cell development. *Development* **126**, 3425–3436 (1999).
19. D. M. Parichy, D. G. Ransom, B. Paw, L. I. Zon, S. L. Johnson, An orthologue of the *kit*-related gene *fms* is required for development of neural crest-derived xanthophores and a subpopulation of adult melanocytes in the zebrafish, *Danio rerio*. *Development* **127**, 3031–3044 (2000).
20. S. S. Lopes *et al*., Leukocyte tyrosine kinase functions in pigment cell development. *PLoS Genet.* **4**, e1000026 (2008).
21. B. Wehrle-Haller, J. A. Weston, Altered cell-surface targeting of stem cell factor causes loss of melanocyte precursors in Steel17H mutant mice. *Dev. Biol.* **210**, 71–86 (1999).
22. T. O'Reilly-Pol, S. L. Johnson, Kit signaling is involved in melanocyte stem cell fate decisions in zebrafish embryos. *Development* **140**, 996–1002 (2013).
23. J. F. Rawls, S. L. Johnson, Temporal and molecular separation of the kit receptor tyrosine kinase's roles in zebrafish melanocyte migration and survival. *Dev. Biol.* **262**, 152–161 (2003).
24. J. A. Lister, C. P. Robertson, T. Lepage, S. L. Johnson, D. W. Raible, Nacre encodes a zebrafish microphthalmia-related protein that regulates neural-crest-derived pigment cell fate. *Development* **126**, 3757–3767 (1999).
25. C. Levy, M. Khaled, D. E. Fisher, MITF: Master regulator of melanocyte development and melanoma oncogene. *Trends Mol. Med.* **12**, 406–414 (2006).
26. S. L. Johnson, A. N. Nguyen, J. A. Lister, Mitfa is required at multiple stages of melanocyte differentiation but not to establish the melanocyte stem cell. *Dev. Biol.* **350**, 405–413 (2011).
27. Z. Zeng, S. L. Johnson, J. A. Lister, E. E. Patton, Temperature-sensitive splicing of mitfa by an intron mutation in zebrafish. *Pigment Cell Melanoma Res.* **28**, 229–232 (2015).
28. D. Gur *et al*., The dual functional reflecting Iris of the Zebrafish. *Adv. Sci. (Weinh.)* **5**, 1800338 (2018).
29. M. Hirata, K. Nakamura, T. Kanemaru, Y. Shibata, S. Kondo, Pigment cell organization in the hypodermis of zebrafish. *Dev. Dyn.* **227**, 497–503 (2003).
30. D. Gur, B. A. Palmer, S. Weiner, L. Addadi, Light manipulation by guanine crystals in organisms: Biogenic scatterers, mirrors, multilayer reflectors and photonic crystals. *Adv. Funct. Mater.* **27**, 1603514 (2016).
31. A. Hirsch *et al*., "Guanigma": The revised structure of biogenic anhydrous guanine. *Chem. Mater.* **27**, 8289–8297 (2015).
32. X. Qiu *et al*., Single-cell mRNA quantification and differential analysis with Census. *Nat. Methods* **14**, 309–315 (2017).
33. E. Becht *et al*., Dimensionality reduction for visualizing single-cell data using UMAP. *Nat. Biotechnol.* 10.1038/nbt.4314 (2018).
34. S. Fukamachi, M. Sugimoto, H. Mitani, A. Shima, Somatolactin selectively regulates proliferation and morphogenesis of neural-crest derived pigment cells in medaka. *Proc. Natl. Acad. Sci. U.S.A.* **101**, 10661–10666 (2004).
35. J. M. Odiorne, The occurrence of guanophores in Fundulus. *Proc. Natl. Acad. Sci. U.S.A.* **19**, 750–754 (1933).
36. E. F. Fries, White pigmentary effectors (leucophores) in killifishes. *Proc. Natl. Acad. Sci. U.S.A.* **28**, 396–401 (1942).
37. A. V. Kalueff *et al*.; Zebrafish Neuroscience Research Consortium, Towards a comprehensive catalog of zebrafish behavior 1.0 and beyond. *Zebrafish* **10**, 70–86 (2013).
38. P. Salis *et al*., Developmental and comparative transcriptomic identification of iridophore contribution to white barring in clownfish. *Pigment Cell Melanoma Res.* **32**, 391–402 (2019).
39. L. W. Oliphant, J. Hudon, Pteridines as reflecting pigments and components of reflecting organelles in vertebrates. *Pigment Cell Res.* **6**, 205–208 (1993).
40. I. Ziegler, The pteridine pathway in zebrafish: Regulation and specification during the determination of neural crest cell-fate. *Pigment Cell Res.* **16**, 172–182 (2003).
41. M. C. Niu, Further studies on the origin of amphibian pigment cells. *J. Exp. Zool.* **125**, 199–220 (1954).
42. E. Dupin, C. Real, C. Glavieux-Pardanaud, P. Vaigot, N. M. Le Douarin, Reversal of developmental restrictions in neural crest lineages: Transition from Schwann cells to glial-melanocytic precursors in vitro. *Proc. Natl. Acad. Sci. U.S.A.* **100**, 5229–5233 (2003).
43. K. Takahashi, S. Yamanaka, A decade of transcription factor-mediated reprogramming to pluripotency. *Nat. Rev. Mol. Cell Biol.* **17**, 183–193 (2016).
44. T. Sandoval-Guzmán *et al*., Fundamental differences in dedifferentiation and stem cell recruitment during skeletal muscle regeneration in two salamander species. *Cell Stem Cell* **14**, 174–187 (2014).
45. A. J. Merrell, B. Z. Stanger, Adult cell plasticity in vivo: De-differentiation and transdifferentiation are back in style. *Nat. Rev. Mol. Cell Biol.* **17**, 413–425 (2016).
46. R. L. Mort, I. J. Jackson, E. E. Patton, The melanocyte lineage in development and disease. *Development* **142**, 620–632 (2015).
47. P. Salis *et al*., Ontogenetic and phylogenetic simplification during white stripe evolution in clownfishes. *BMC Biol.* **16**, 90 (2018).
48. C. M. Garcia, E. Ramirez, Evidence that sensory traps can evolve into honest signals. *Nature* **434**, 501–505 (2005).
49. A. Kodric-Brown, Female preference and sexual selection for male coloration in the guppy (Poecilia reticulata). *Behav. Ecol. Sociobiol.* **17**, 199–205 (1985).
50. M. R. Lang, L. B. Patterson, T. N. Gordon, S. L. Johnson, D. M. Parichy, Basonuclin-2 requirements for zebrafish adult pigment pattern development and female fertility. *PLoS Genet.* **5**, e1000744 (2009).

Supplementary Information for

Fate plasticity and reprogramming in genetically distinct populations of *Danio* leucophores

Victor M. Lewis[a,b], Lauren M. Saunders[a,c,d], Tracy A. Larson[a], Emily J Bain[a], Samantha L. Sturiale[a], Dvir Gur[e,f], Sarwat Chowdhury[g], Jessica D. Flynn[h], Michael C. Allen[i], Dimitri D. Deheyn[i], Jennifer C. Lee[h], Julian A. Simon[g], Jennifer Lippincott-Schwartz[e], David W. Raible[b,j], and David M. Parichy[a,k,1]

[a] Department of Biology, University of Virginia, Charlottesville, VA 22903
[b] Department of Biology, University of Washington, Seattle, WA 98195
[c] Department of Genome Sciences, University of Washington, Seattle, WA 98195
[d] Program in Molecular and Cellular Biology, University of Washington, Seattle, WA 98195
[e] Janelia Research Campus, Howard Hughes Medical Institute, Ashburn, Virginia 20147
[f] Eunice Kennedy Shriver National Institute for Child Health and Human Development, National Institutes of Health, Bethesda, MD 20892
[g] Clinical Research Division of Molecular Pharmacology, Fred Hutchinson Cancer Research Center, Seattle, WA 98109
[h] National Heart, Lung, and Blood Institute, National Institutes of Health, Bethesda, MD 20892
[i] Marine Biology Research Division, Scripps Institution of Oceanography, University of California San Diego, La Jolla, California 92093
[j] Department of Biological Structure, University of Washington, Seattle, WA 98195
[k] Department of Cell Biology, University of Virginia, Charlottesville, VA 22903

[1]To whom correspondence should be addressed. Email: dparichy@virginia.edu.

Supplementary Information Text

Fig. S1. Widespread distribution of leucophores in fins of adult *Danio*. (*A*) Phylogenetic relationships of select *Danio* [after (1)] indicating presence in anal and dorsal fins of leucophores either containing white and orange pigment ("xantholeucophores") or white and occasional black pigment ("melanoleucophores," see Main Text). Only *D. erythromicron* lacked such cells entirely. For images of whole fish see (2). (*B*) Xantholeucophores in the anal fin and melanoleucophores in the dorsal fin of *D. rerio*. Upper panels show morphologies of cells in fish housed in standard rearing conditions. Lower panels show cellular phenotypes following treatment with epinephrine. Examples of xantholeucophores are indicated with yellow circles, white melanoleucophores with cyan circles, and melanoleucophores also containing melanin with dashed cyan circles. Green box, iridescent iridophores. Red arrow, contracted pigment of xanthophore, lacking discernible white material. (*C*) Xantholeucophores and melanoleucophores, or their absence, in fins of other *Danio* shown in *A*. Both leucophore classes were evident in anal fins of *D. nigrofasciatus* and *D. choprae*, with melanoleucophores located distally and xantholeucophores more proximally. The orange or yellow cast to anal fin melanoleucophores in *D. nigrofasciatus* and *D. choprae* results from co-occurring presumptive xanthophores (pigment accumulations of individual xanthophores are not apparent in this image of *D. choprae*). Xantholeucophores were evident in dorsal fins of *D. kyathit* and *D. tinwini*, yet had less distinctive accumulations of white material than xantholeucophores of anal fins. Yellow arrows in C indicate pigment accumulations of yellow/orange xanthophores or red erythrophores. In *D. erythromicron*, an asterisk indicates whitish debris of unknown origin. Other annotations as in *B*. (Scale bar in *B* for *B* and *C*, 50 μm)

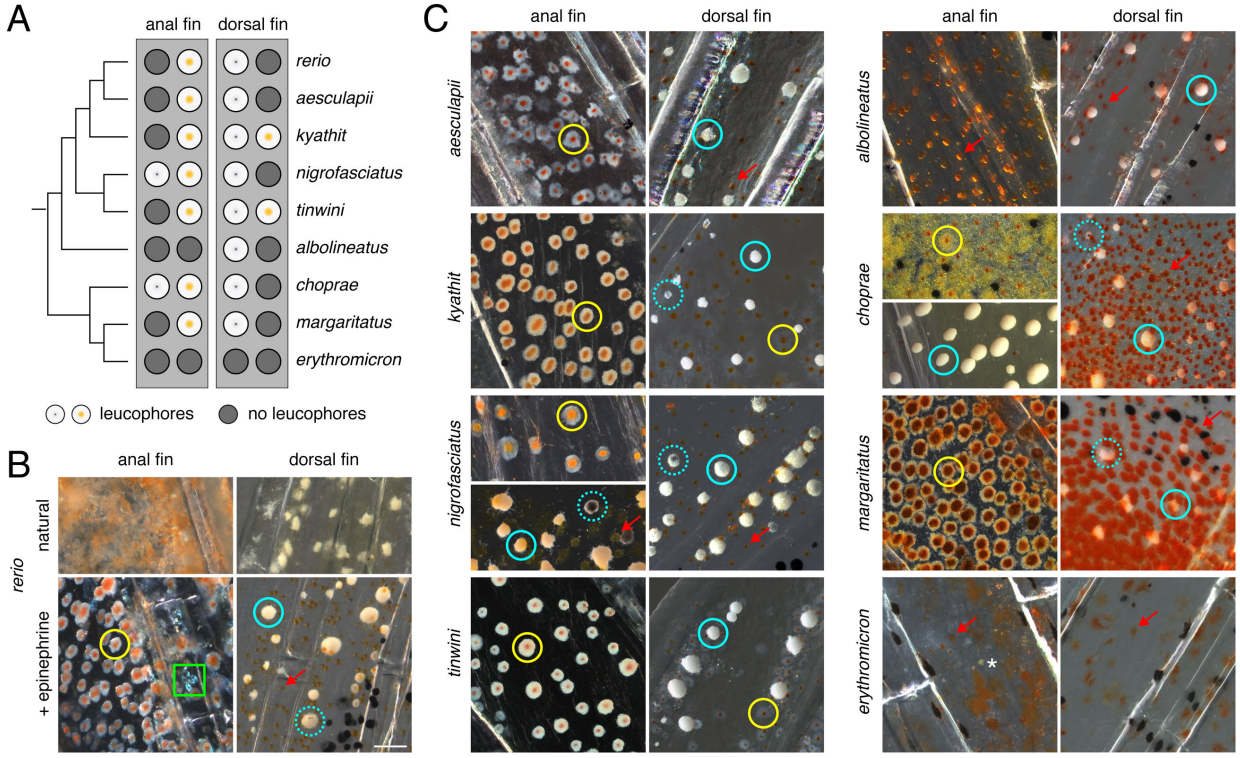

Fig. S2. Pigmentary components of xantholeucophores and first appearance. (*A*) Similar to xanthophores, leucophores of the anal fin (xantholeucophores) contained pteridines (3), revealed by autofluorescence under DAPI illumination in response to dilute ammonia treatment (4). Before administration of ammonia (pre-NH_4^+), no fluorescence was detectable at this magnification and exposure. After ammonia treatment (post-NH_4^+), xantholeucophores exhibited strong autofluorescence whereas leucophores of the dorsal fin (melanoleucophores) did not exhibit autofluorescence. Image exposure times were the same before and after treatment and between cell types. (*B*) Yellow-orange coloration of anal fin xantholeucophores is carotenoid-based, as indicated by the absence of such color in zebrafish mutants for *scarb1*, a gene essential for carotenoid localization (5, 6). Dorsal fin melanoleucophores were indistinguishable between wild-type and *scarb1* mutant fish. Arrowhead, iridophore. (*C*) High resolution image of xantholeucophore plated *ex vivo*, reveals carotenoid vesicles and background autofluorescence (green) with weak autofluorescence centrally in DAPI channel (blue). Treatment of the same cell with dilute ammonia induced widespread autofluorescence (blue) indicative of pteridine release. (*D*) Xantholeucophore appearance in *D. aesculapii* [PR stage (7)].Images on day 1 (d1) indicate two representative, orange-pigment containing xanthophore-like cells, and their broader tissue context. One cell (arrowhead) migrated from the field of view whereas another, cell (1) exhibited distinctive white pigment by d3. A second newly appearing cell (2) on d3 had clearly evident white pigment by d5. (*E*) Xantholeucophore differentiation in *D. rerio*. (Scale bars: *A*, 50 µm; *B*, 20 µm; *C*, 10 µm; *E*, 200 µm)

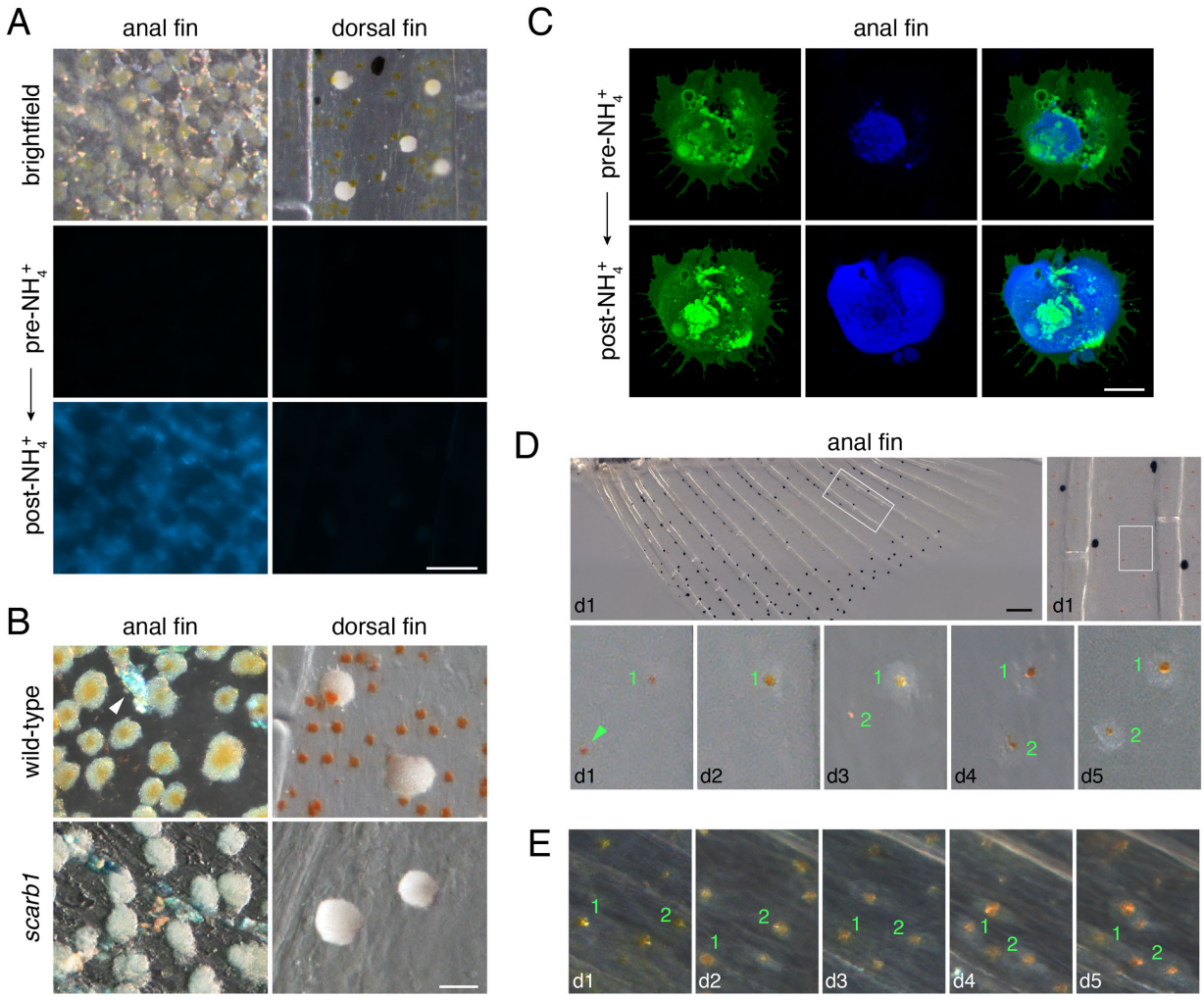

Fig. S3. Reporter labeling. (*A*) Brightfield and fluorescence images for *aox5*:palm-EGFP and *pnp4a*:palm-mCherry. For dorsal fin, asterisks indicate *aox5* transgene expression by xanthophores adjacent to a melanoleucophore. Melanoleucophores did not express *aox5*:palm-EGFP as indicated by the absence of membrane-targeted EGFP fluorescence in cell peripheries, though deposits of white material at cell centers reflected light in green channel. (*B*) Mosaic expression of *tyrp1b* transgene in melanoleucophores. Arrowheads, two cells that expressed the transgene as evidenced by membrane-targeted palm-mCherry expression. Cells with small amounts of white pigment and some melanin often expressed *tyrp1b*:palm-mCherry (arrowheads), whereas cells having larger accumulations of white pigment and no melanin (asterisks) failed to express detectable levels of reporter. Green channel (no fluorophore) reveals reflectance from white deposits of melanoleucophores (also evident in red channel) and endogenous autofluorescence of carotenoids in xanthophores. (*C*) High resolution images of melanoleucophore and xantholeucophore plated *ex vivo* illustrate expression of *pnp4a* transgene by both cell types but xantholeucophore-specific expression of *aox5*. Arrowhead, compacted, autofluorescing carotenoids (contained within carotenoid vesicles) contracted to cell center by epinephrine. Blue, DAPI-labeled nuclei. Note that some cell shape change is evident between bright-field and fluorescence images, which were acquired on different microscopes. Approximate boundaries of xantholeucophore are outlined for clarity in brightfield. (Scale bars: *A*, 20 µm; *B*, µm; *C*, 10 µm)

(figure on next page)

Fig. S3.

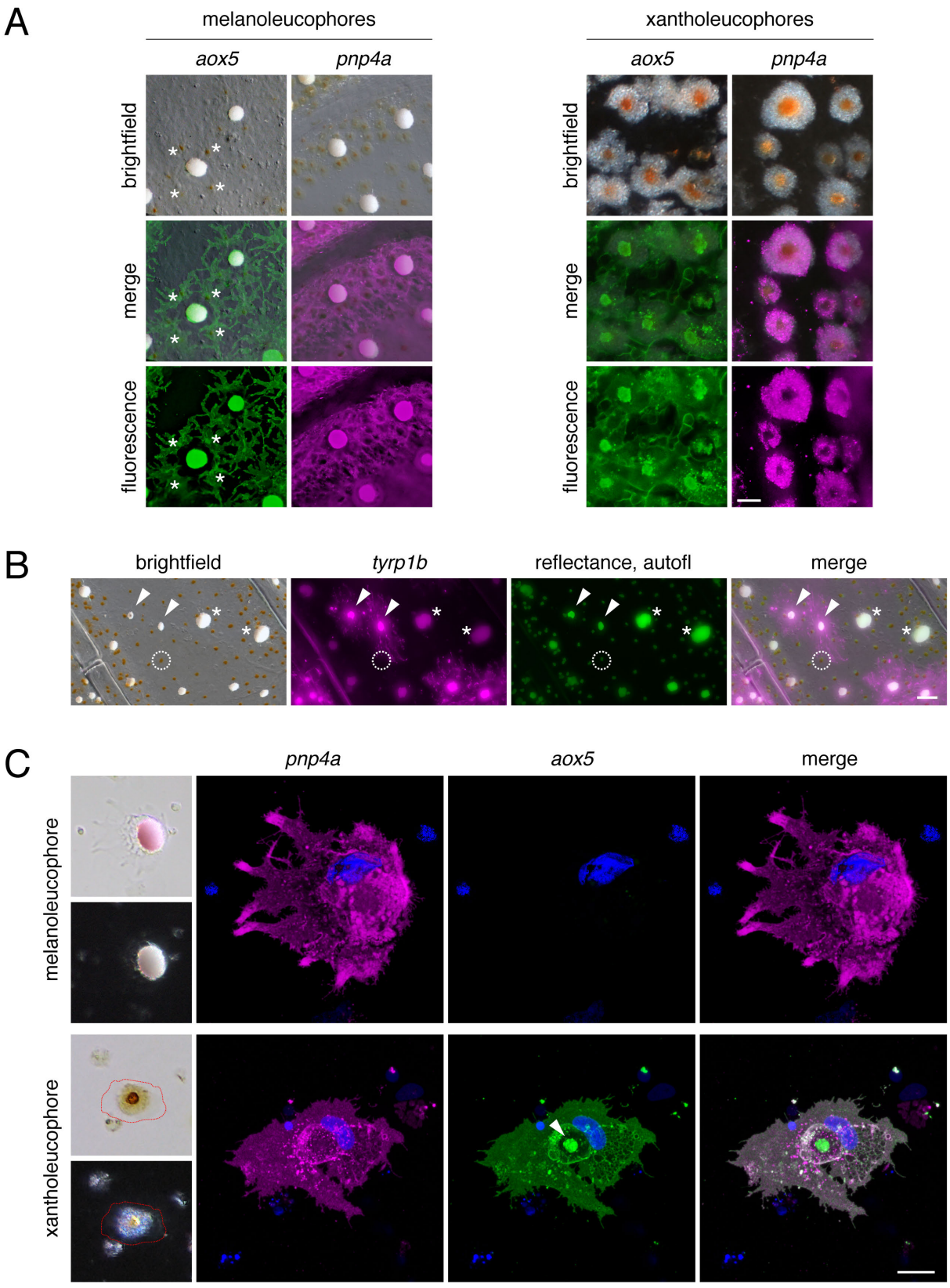
A
melanoleucophores
xantholeucophores
aox5
pnp4a
aox5
pnp4a
brightfield
merge
fluorescence
brightfield
merge
fluorescence
B
brightfield
tyrp1b
reflectance, autofl
merge
C
pnp4a
aox5
merge
melanoleucophore
xantholeucophore

Fig. S4. Genetic requirements of melanoleucophores and xantholeucophores. (*A)* In *D. rerio*, fish mutant for a presumptive null allele of *csf1ra* (8) retained melanoleucophores, while lacking xanthophores. By contrast, melanoleucophores were absent from fish mutant for a null allele of *kita*, in which melanophores are deficient (9). Mutants exhibited reciprocal phenotypes for xantholeucophores, which were lost in the *csf1ra* mutant, but persisted in the *kita* mutant. An *ltk* mutant, completely lacking iridophores (10), retained both leucophore classes. (*B*) *D. aesculapii* mutant phenotypes were concordant with those of *D. rerio*. It was not feasible to test genetic requirements of leucophores for *ltk* in *D. aesculapii* owing to lethality of null alleles (10). (*C*) In mutants homozygous for presumptive null alleles of *mitfa* (11), melanoleucophores were lost in addition to melanophores. Unexpectedly, given requirements for Mitfa in melanophore but not xanthophore development (11), *mitfa* mutants had a xantholeucophore defect in which yellow/orange cells in the position of xantholeucophores lacked white pigmentation. *mitfa* mutants also lacked fin iridophores, despite the persistence of these cells on the body (11). Insets, cells with yellow or orange pigment that may be xanthophores or white-pigment free xantholeucophores. (*D*) Summary of fin pigmentation phenotypes. Asterisk, melanophores occur sparsely in proximal regions of caudal fin and body of *D. rerio kita* mutants (9, 12).

(figure on next page)

Fig. S4.

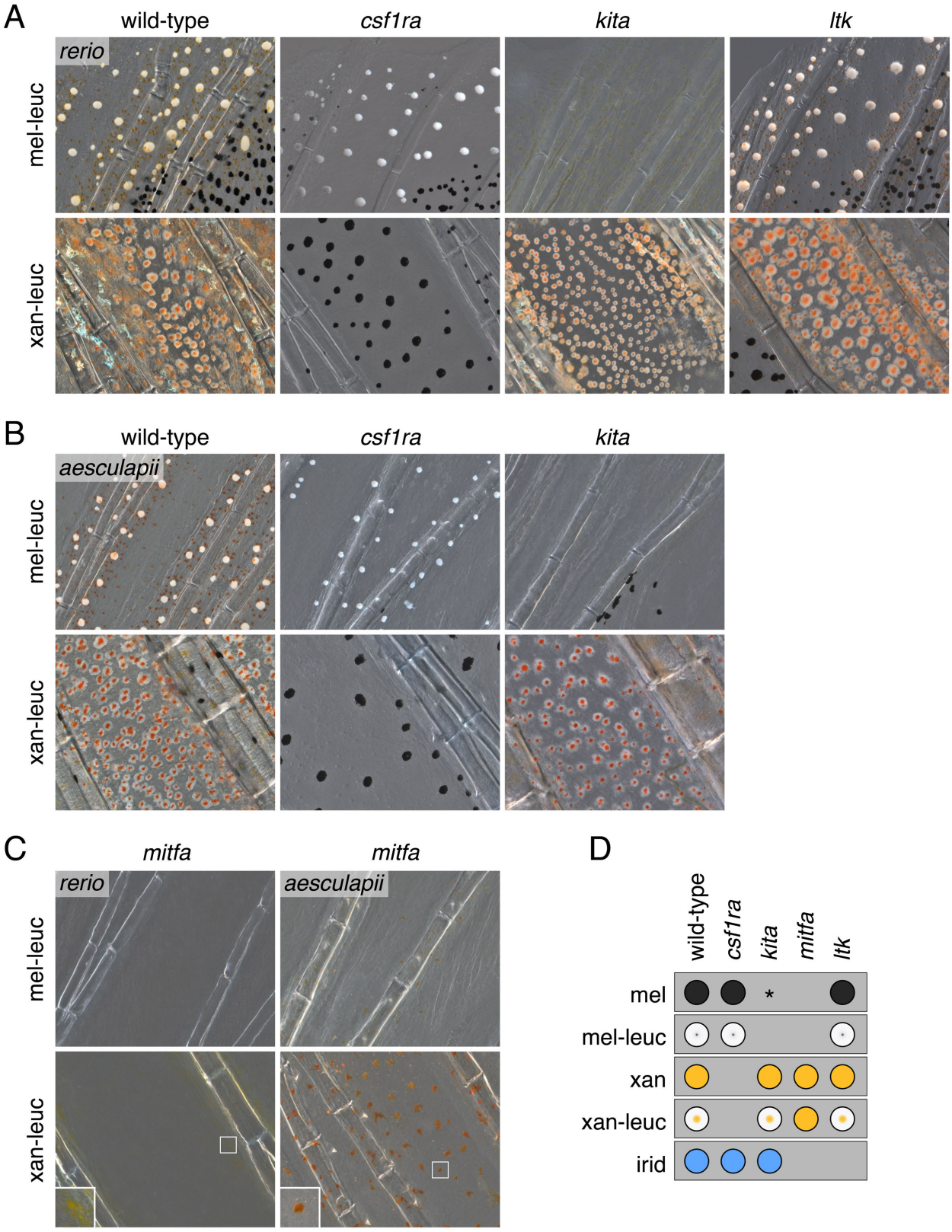
A
wild-type
csf1ra
kita
ltk
rerio
mel-leuc
xan-leuc
B
wild-type
csf1ra
kita
aesculapii
mel-leuc
xan-leuc
C
mitfa
mitfa
rerio
aesculapii
mel-leuc
xan-leuc
D
wild-type
csf1ra
kita
mitfa
ltk
mel
mel-leuc
xan
xan-leuc
irid

Fig. S5. Physical and chemical characteristics of melanoleucophores and xantholeucophores. (*A Upper*) Hyperspectral imaging of melanoleucophores revealed high, nearly uniform reflectance (refl) across visible wavelengths and correspondingly low transmittance (trans). (*A Lower*) Hyperspectral imaging of xantholeucophores was performed across regions devoid of carotenoid (solid lines) and regions in which carotenoids had been contracted to cell centers by epinephrine (dotted lines). Reduced reflectance and transmittance below ~550 nm are consistent with the presence of pteridines and carotenoids not found in melanoleucophores. (*B*) Xanthophores and xantholeucophores each contained presumptive pterinosomes (p) and carotenoid vesicles (c). Organelle sizes were variable within and between cell types. (*C–E*) Mass spectrometry. (*C*) Purine standards (left; h, hypoxanthine; g, guanine; x, xanthine; u, uric acid) and fin regions excised (right). From dorsal fin, distal tissues normally harboring melanoleucophores and proximal tissue lacking melanoleucophores were compared between one another and between genetic backgrounds with or without melanoleucophores. From anal fin tissue, regions normally harboring xantholeucophores (and in some cases iridophores) were combined and then compared between genetic backgrounds with differing complements of these cells. (*D*) Supplementary mass spectrometric analysis of dorsal fin tissue with and without melanoleucophores confirmed an association of melanoleucophores and guanine excess. Positions of standards identified in *C* are shown with vertical dashed red lines. Plots *D-1* and *D-2* indicate illustrate guanine (g) peak (arrowhead) in distal fin tissue containing melanoleucophores of wild-type *D. rerio* (same as Fig. 2*E*—upper) and loss of this peak from the same distal fin region when melanoleucophores were ablated genetically in the *mitfa* mutant (*SI Appendix* Fig. S4*C*). *D-3* and *D-4* illustrate for *D. aesculapii* the co-occurrence of excess guanine (arrowhead) in distal fin tissue containing melanoleucophores and the lack of a guanine signature in more proximal fin tissue lacking melanoleucophores as in *D. rerio* (compare to Fig. 3*E*). (*E*) Mass spectrometric analysis of anal fin tissue revealed a guanine signature less pronounced than for melanoleucophores, dependent on the presence of both xantholeucophores and co-occurring iridophores. Plot *E-1* shows guanine (arrowhead) in fin tissue containing both xantholeucophores and iridophores of wild-type *D. rerio*. *E-2*, A diminished guanine signature was evident in tissue containing xantholeucophores but not iridophores of *ltk* mutant *D. rerio* (*SI Appendix* Fig. S4*A*). *E-3*, The guanine signature was absent from tissue lacking both xantholeucophores and iridophores of *mitfa* mutant *D. rerio*. *E-4*, A guanine signature was evident in tissue containing both xantholeucophores and iridophores of wild-type *D. aesculapii*, as in *D. rerio*. Consistent with relatively low levels of guanine independent of iridophores in anal fin tissue, Raman spectroscopy failed to identify a signature of guanine in individual xantholeucophores (Fig. 3*F*). Leucophores of medaka fish are thought to depend on uric acid for their white appearance (13), yet substantial quantities of uric acid (u, in plots) were not detected in either melanoleucophores or xantholeucophores of *Danio*. (Scale bar in *B*, 500 nm)

(figure on next page)

Fig. S5

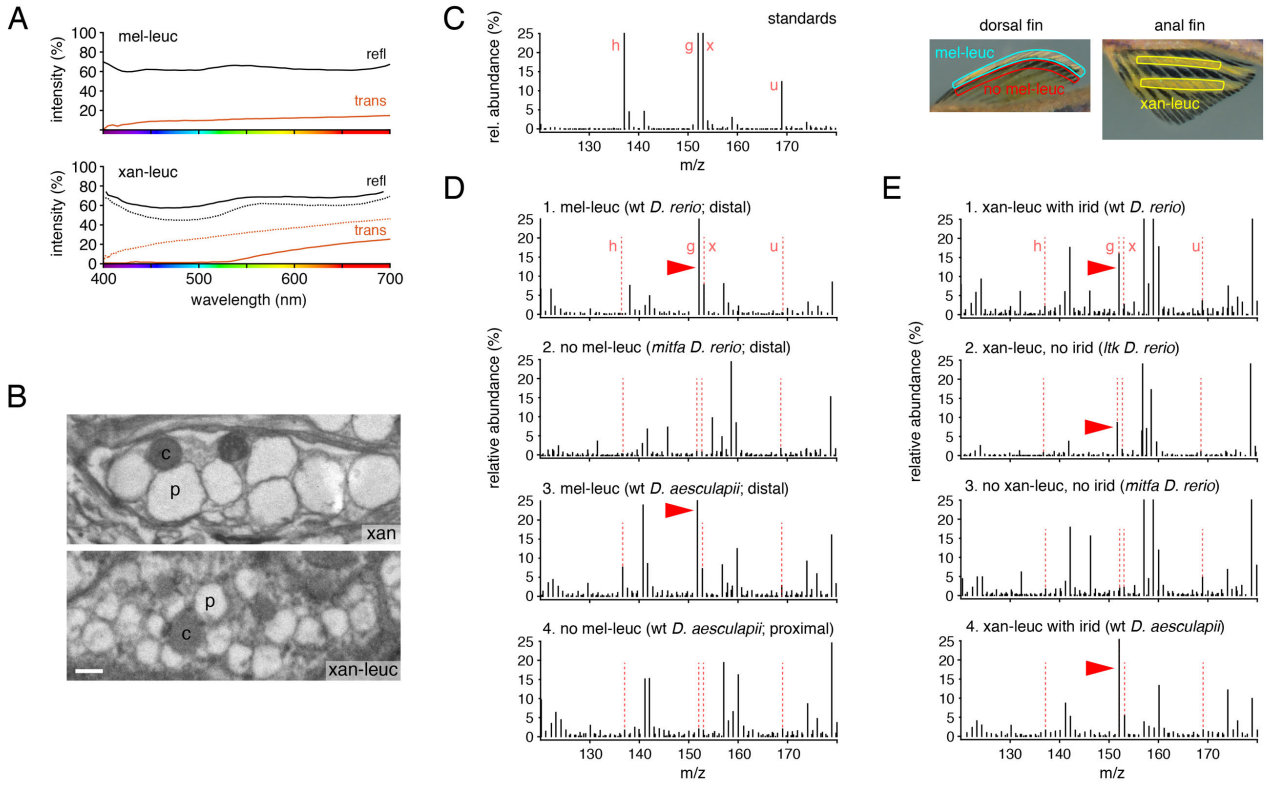
A
mel-leuc
refl
trans
intensity (%)
xan-leuc
wavelength (nm)
B
c
p
xan
xan-leuc
C
standards
rel. abundance (%)
h
g
x
u
m/z
dorsal fin
anal fin
mel-leuc
no mel-leuc
xan-leuc
D
1. mel-leuc (wt D. rerio; distal)
2. no mel-leuc (mitfa D. rerio; distal)
3. mel-leuc (wt D. aesculapii; distal)
4. no mel-leuc (wt D. aesculapii; proximal)
relative abundance (%)
E
1. xan-leuc with irid (wt D. rerio)
2. xan-leuc, no irid (ltk D. rerio)
3. no xan-leuc, no irid (mitfa D. rerio)
4. xan-leuc with irid (wt D. aesculapii)

Fig. S6. Population characteristics and clustering of single cell RNA-sequencing (scRNA-Seq) data set from zebrafish fin. (*A*) UMAP representation of all cells collected (*N*=4599) with identities of major clusters inferred by expression of known markers, including cells of epidermis, dermal skeleton, and the immune system as well as xanthophores or xantholeucophores (x/x-l) and melanophores or melanoleucophores (m/m-l). Iridophores are fragile and did not persist through cell dissociation; therefore few were recovered in these analyses. (*B*) Counts of unique expressed genes, unique molecular identifiers (UMI) and fractions of mitochondrial reads by cell type. Relatively low proportions of mitochondrial genes observed here are consistent with intact rather than broken cells (14). Plots show medians with boxes spanning interquartile ranges; vertical lines indicate farthest observations with outliers depicted individually. (*C*) UMAP representation of pigment cell clusters inferred by molecular marker expression to represent xanthophores (x), xantholeucophores (x-l), melanophores (m) and melanoleucophores (m-l). (Same plot as Fig. 4*B-left*.) Numbers in parenthesis indicate total cells comprising each cluster. Arrow indicates cells bridging melanophore and melanoleucophore clusters. Dashed lines indicate lack of cells occupying space between xanthophores (derived from dorsal fin) and xantholeucophores (derived from anal fin). (*D*,*E*) *Post hoc* verification of cluster cell-type assignments by comparison of visually confirmed cellular phenotypes and gene expression. Bubble plot in *D* illustrates mean expression level and proportion of cells expressing each of 4 candidate marker loci across the 4 pigment cell clusters identified by scRNA-Seq and UMAP clustering. Areas of bubbles indicate fractions of cells expressing each gene and colors indicate normalized expression levels (scales are shown to right of plot). RT-PCR in *E* illustrates expression of same marker loci in cells of each class picked manually *in vitro*, as well as whole fin tissue (RT–, fin tissue prepared without reverse transcriptase). (*F–I*) Gene expression mapped to UMAP representation of cell clusters. (*F*) Genes corresponding to reporters used in this study. Breadth of *pnp4a* and *mitfa* expression were consistent with independent observations (5). (*G*) Genes used in *post hoc* validation of cell-type assignments (*D,E*). (*H*) Genes corresponding to mutants used in this study (*csf1ra* expression was not detectable by scRNA-Seq). (*I*) Genes identified for roles in early larval leucophore development in medaka. *slc2a11b* corresponds to medaka *white leucophore* (*wl*), required for the development of yellow coloration in both xanthophores and leucophores. *slc2a15b* (*leucophore free*, *lf*), is required for both leucophore and xanthophore development from early stages. *sox5* (*many leucophores*, *ml-3*) promotes the development of xanthophores over leucophores. *pax7a* (*lf-2*) is required for the development of most leucophores and all xanthophores. None of the medaka leucophore-associated genes exhibited strongly type-specific expression in zebrafish adult fin pigment cells.

(figure on next page)

Fig. S6.

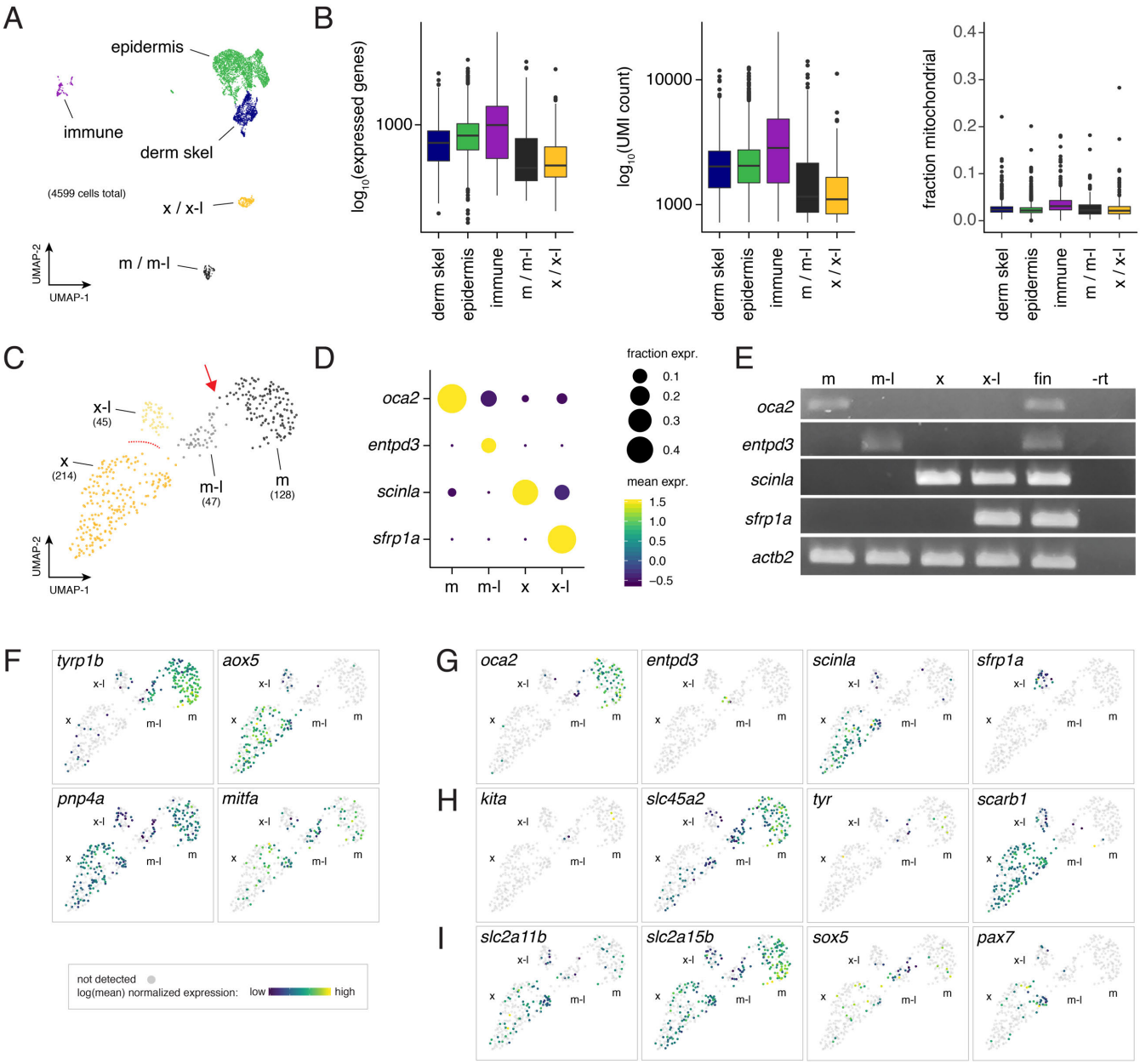
A
epidermis
immune
derm skel
(4599 cells total)
x / x-l
m / m-l
UMAP-2
UMAP-1
B
log10(expressed genes)
1000
log10(UMI count)
10000
1000
fraction mitochondrial
0.4
0.3
0.2
0.1
0.0
derm skel
epidermis
immune
m / m-l
x / x-l
C
x-l
(45)
x
(214)
m-l
(47)
m
(128)
UMAP-2
UMAP-1
D
oca2
entpd3
scinla
sfrp1a
m
m-l
x
x-l
fraction expr.
0.1
0.2
0.3
0.4
mean expr.
1.5
1.0
0.5
0.0
−0.5
E
m
m-l
x
x-l
fin
-rt
oca2
entpd3
scinla
sfrp1a
actb2
F
tyrp1b
aox5
pnp4a
mitfa
not detected
log(mean) normalized expression:
low
high
G
oca2
entpd3
scinla
sfrp1a
H
kita
slc45a2
tyr
scarb1
I
slc2a11b
slc2a15b
sox5
pax7

Fig. S7. scRNA-Seq and genetic pathway analysis of melanoleucophore differentiation and xantholeucophores relative to xanthophores (*A*) Melanin-free *D. rerio* mutants of *tyrosinase* (*tyr*) and *albino* (*slc45a2*) had normal complements of leucophores. (*B*) Pseudotemporal ordering of xanthophores (x) and xantholeucophores (x-l) revealed few cells where an intermediate state might be found (red dotted line). Most xanthophores were collected from dorsal fin whereas xantholeucophores were collected from anal fin. (*C*,*D*) Aggregate expression scores (*C*) and individual expression profiles (*D*) for genes of purine, carotenoid and pteridine pathways in xanthophores and xantholeucophores compared to non-pigment cells (np). Different letters above bars indicate means significantly different in *post hoc* comparisons (all $P<0.001$), though comparisons of xanthophores and xantholeucophores are confounded by potential differences in maturation times and rates. Guanosine triphosphate is the most basal substrate for pteridine synthesis (3) so higher expression of purine synthesis genes by xanthophores and xantholeucophores compared to non-pigment cells is expected. (Scale bar, 250 µm)

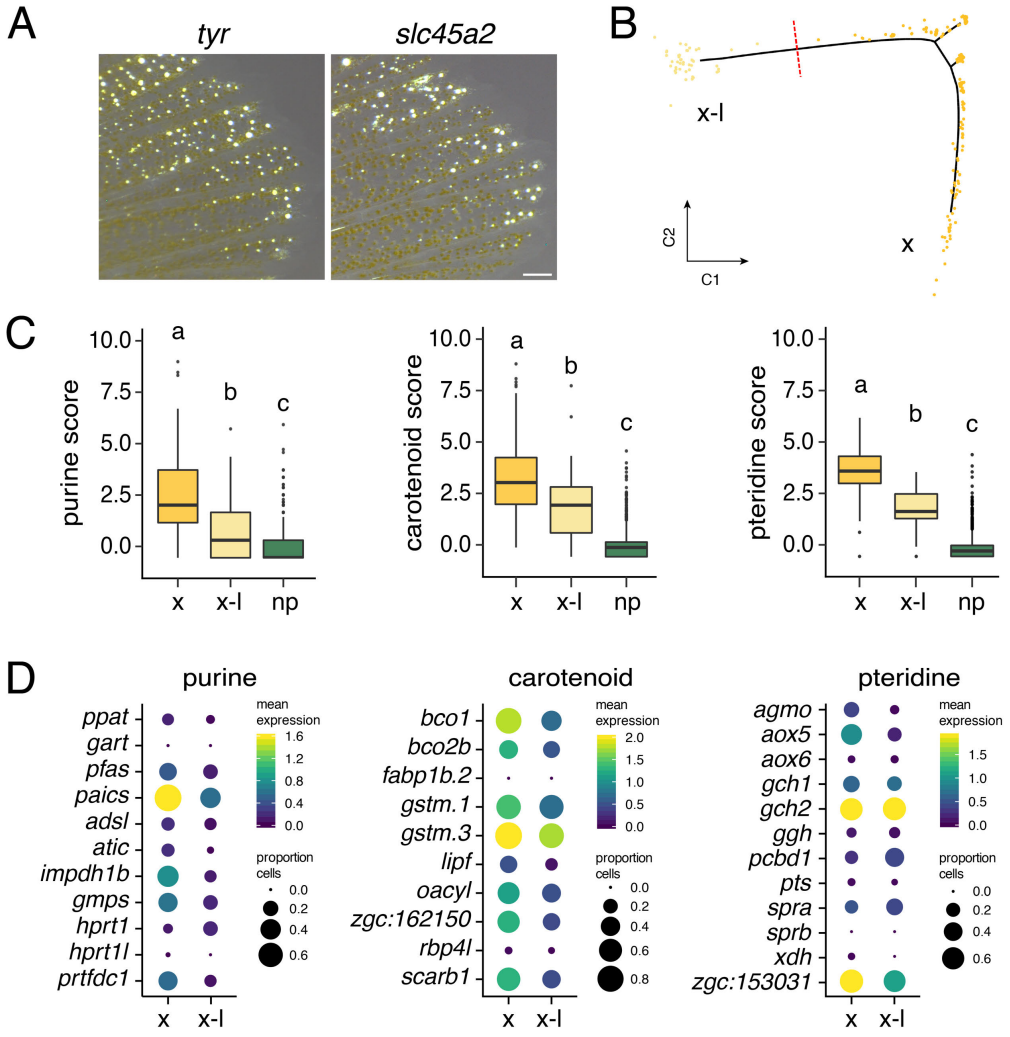

Fig. S8. Behavioral responses to melanoleucophore complement. (*A*) Preliminary experiments confirmed suitability of test arena, as fish spent more time in association with a stimulus compartment containing a shoal of fish than a stimulus compartment without fish (difference in time spent between fish and no-fish compartments, null hypothesis $\Delta t = 0$, two-tailed, t_{28}=7.71, P<0.0001). Each set of points connected by a line indicates times spent by an individual fish in proximity to one or another stimulus shoal compartment and bars indicate means ± 95% CI. Analyses of variance did not reveal differences in times spent shoaling associated with sex of test fish, shoaling fish, or interactions between the two (all P>0.4). (*B*) Examples of stimulus fish as presented to test fish in behavioral trials, following sham-manipulation (intact) or excision of melanoleucophore-containing fin tissue (ablated) two days prior to testing. Arrows indicate locations of cuts without tissue removal whereas arrowheads indicate regions from which tissue was removed (see *SI Appendix* Materials & Methods). (*C*) Despite test fish preferring to shoal in proximity to fish with intact melanoleucophores, first approach varied with melanoleucophore status and sex. Shown are proportions of responses in which test fish, given a choice of phenotypes, first approached either sham-manipulated stimulus fish (ML+) from which non-melanoleucophore containing fin tissue had been removed, or stimulus fish that had been sham-manipulated (ML–). Sex-specificity of approach responses might reflect tendencies of fish to avoid aggressive or other interactions when first encountering an opposite-sex shoal, though such effects will require dedicated experiments to discern. Numbers of fish showing a given response are indicated within bars. Overall heterogeneity among groups, χ^2=17.2, P<0.001, d.f.=3.

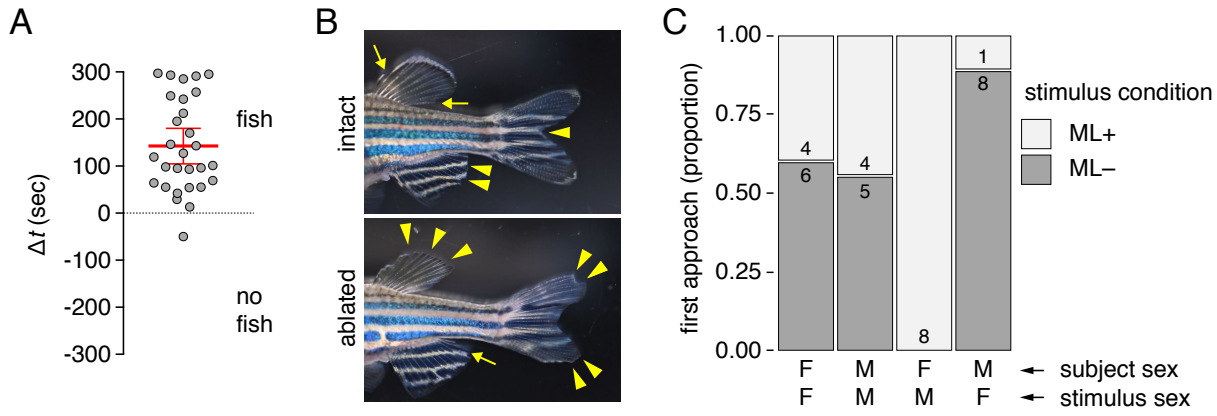

Fig. S9. Summary of observations. (*A*) Integrated results from this study (red) and prior studies of the caudal fin [black; (15, 16)]. Dotted lines are hypothetical. *Danio* xantholeucophores (XL) and melanoleucophores (ML) arise from different sublineages, likely having a common progenitor (XM) (15, 16) that gives rises to xanthophores (X) and melanophores (M). Xantholeucophores acquire distinct yellow/orange pigment before accumulating white pigment, consistent with a conversion of xanthophores (X; i), though our observations do not exclude their differentiation as a distinct cell type directly from unpigmented xanthoblasts (Xb; ii), or a neural crest sublineage independent of XM (not illustrated). Melanoleucophores, however, arise directly from melanophores (iii). Each leucophore lineage is constrained by prior lineage requirements (*csf1ra*; *kita*, *mitfa*), yet melanoleucophore and xantholeucophore specific roles for *mitfa* were identified, as was a melanoleucophore-specific role for *kita*. Differentiation of melanoleucophores further involved reduced expression of melanin pathway genes and loss of melanin by still unknown mechanisms, and the simultaneous upregulation of *de novo* purine synthesis genes, with deposition of crystalline guanine. Both leucophores responded in the context of background adaptation, and melanoleucophore complement was associated with differences in approach and shoaling behavior, raising the possibility of ecological roles in nature. (*B*) Pigment organelle morphologies and arrangements in light-reflecting pigment cells suggest parallel evolution of white pigment phenotype. Stacked reflecting platelets of iridophores (e.g., *Danio*) are responsible for iridescence, whereas stacked, but radially arranged platelets [*Amphiprion*; (17)] are associated with a white, rather than iridescent phenotype. By contrast, presumptive guanine-containing organelles of melanoleucophores are irregularly arranged, as are pterinosomes (green) that contain pteridines and the presumptive white pigment of xantholeucophores (orange, carotenoid vesicles).

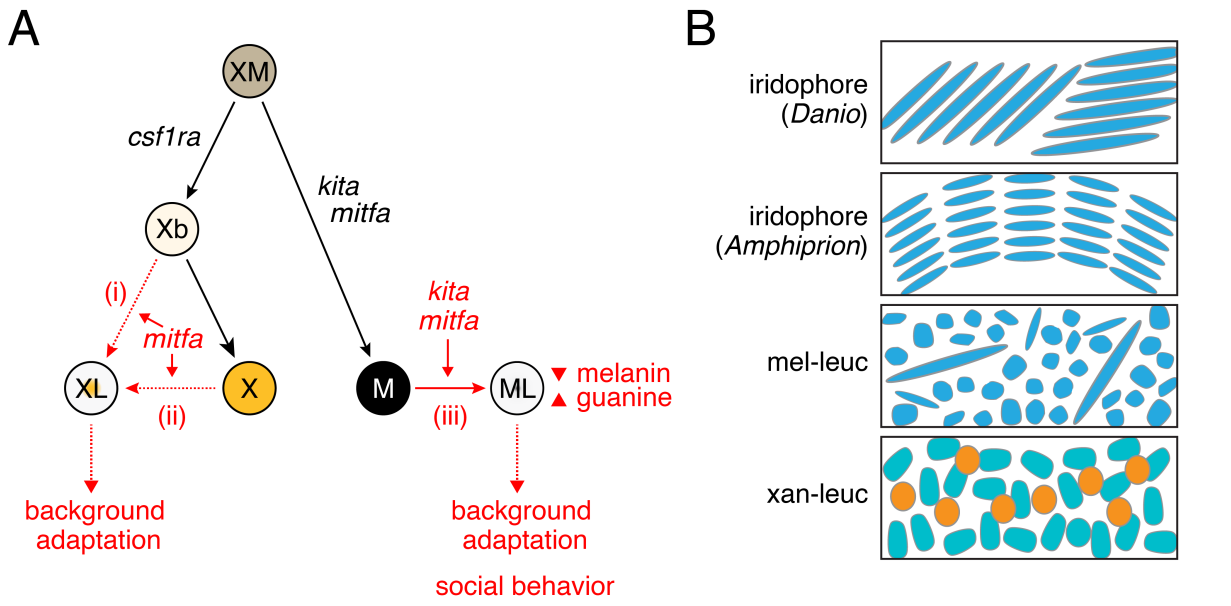

Materials & Methods

Fish Stocks, Staging, Rearing Conditions and Handling

Staging used standardized standard length [SSL; (7)] and fish were at late juvenile or adult stages (>14 SSL) except as indicated. Fish were maintained at ~28.5C with 10 h : 14 h light:dark conditions. Larvae were reared with marine rotifers supplemented with Artemac (Aquafauna) followed by Artemia and flake food. Adults were maintained on Artemia and flake food. Fish stocks of *Danio rerio*: WT(ABb), a derivative of inbred AB^{wp}, *Tg(tyrp1b:palm-mCherry)$^{wp.rt11}$* (18) *Tg(aox5:palmEGFP)$^{wp.rt22}$*(19); *Tg(pnp4a:palmmCherry)$^{wp.rt10}$* (19); *kita^{b5}* (9) *kita^{ji199}* (20) *csf1ra^{j4blue}* (8) *ltk^{j9s1}* (10) *mitfa^{w2}* (11) *mitfa^{vc7}* (21) *scarb1$^{vp.r32c1}$*, *tyr$^{vp.r33c1}$* (5); *slc45a2^{b4}* (22). Wild-type *Danio* species other than *D. rerio* were field-collected or obtained from commercial suppliers and maintained in the laboratory for 1–10 generations. Fish were anesthetized in MS222 prior to clipping fins or imaging. To contract pigment granules for imaging, fish were treated with 1 mg/ml epinephrine for ~5 min. All procedures involving live fish followed federal, state and local guidelines for humane treatment and protocols approved by Institutional Animal Care and Use Committees of University of Virginia and University of Washington.

CRISPR/Cas9 Mutagenesis

One-cell embryos were injected with 200 ng/µl sgRNAs and 500 ng/µl Cas9 protein (PNA Bio) according to standard procedures (23). Guides were tested for mutagenicity by Sanger sequencing and injected fish were reared to maturity at which time they were screened for germline transmission of new mutations. Mutants of *D. aesculapii* generated for studies of adult body pigmentation were F1–F3 progeny of injected fish and heteroallelic for loss of function mutations resembling null alleles of *D. rerio*. sgRNA target sites, excluding PAM were: *csf1ra*, GGATCAGGACACCCTTTCTG, GGTTGTAAAACCTGTTCTCT; *kita*, GGGAAAATATTCATGCCGAG, GGACCTTGTGGGGTAATGGT; *mitfa*, GGGAGGGTGAGAAGGGCCAT, GGGCTCCCAGTGCACTGGAC.

Transgenesis and Lineage Analysis

Tol2 mediated transgenesis followed established methods (24). A *mitfa:tdTomato* construct was generated by Gateway cloning using the Tol2Kit (25) using a 5 kb upstream regulatory region of *mitfa* and *tdTomato*. A *pnp4a:nlsEos* construct was generated by ligation of 9.4 kb *pnp4a* regulatory sequence to nuclear localizing, multimeric EosFP fluorophore. For mosaic injections in clonal labeling and Eos fate mapping, 5 pg plasmid DNA and 20 pg Tol2 mRNA were injected into 1–2 cell embryos (16, 26). For clonal labeling, 494 injected embryos were screened at 5 dpf for tdTomato+ melanophores, yielding 228 (46% of injected) larvae that were reared to 12 SSL before screening again for tdTomato in the dorsal fin, resulting in 64 (13% of injected) individuals, which were then scored for labeled melanophores and melanoleucophores. The infrequent labeling of dorsal fins suggested we had labeled only single clonal lineages and the distributions of these cells, limited to regions of 1–2 fins and extending proximal–distal along the fins, were consistent with prior analyses of clonally related fin pigment cells (15, 16); in only a single individual were labeled pigment cells non-contiguous, occurring at fin rays 2–3 and 5–6, and this fish was excluded from analysis. For Eos-labeling, embryos were screened at 5 dpf for *pnp4a*:Eos+ iridophores then reared in tanks shaded from ambient light to prevent spontaneous photoconversion (19). Eos+ fish were screened again at 8.6 SSL for labeling in the dorsal fin, at which time Eos+ melanophore clones were photoconverted (i.e., green to red).

Imaging
Images were acquired with a Zeiss AxioObserver epifluorescence inverted microscope, a Zeiss LSM 880 laser scanning confocal microscope equipped with Fast Airyscan detector, a AxioZoom V.16 stereomicroscope using Axiocam 506 color cameras, and a Leica M205FA stereomicroscope with Leica DFC550 color camera. Images were adjusted for display level, corrected for color balance, and aligned if necessary to correct for imaging on different platforms in Adobe Photoshop CS. Images from all conditions within each analysis were treated identically.

Image Series and Cell Counts
Fish for daily image series or cell counts were reared individually in glass beakers, treated with epinephrine to contract pigment, anesthetized using MS222, imaged and then allowed to recover. For analyses of dorsal fin melanoleucophores containing melanin, cells were counted from an image series of whole fins. For experiments using *mitfa*^{vc7} and *kita*^{j1e99} temperature-sensitive alleles, melanophores and melanoleucophores were counted manually under incident light.

Temperature Shift Experiments
Temperature shift experiments were conducted using glass tanks either heated with 300V submersible heaters or cooled with a 0.25 HP drop-in chiller. Temperature was regulated using a digital temperature regulator set to maintain ±0.5°C and cross-referenced daily with a second digital thermometer. For temperature-shift experiments using the *mitfa*^{vc7} allele, fish were reared at permissive temperature (25 °C) until melanophores and melanoleucophores had fully populated the distal dorsal fin (9.2 SSL) (21). Melanophores and melanoleucophores were counted and fish were then placed in beakers and shifted to a restrictive temperature (33 °C) for 2 d at which time melanophores and melanoleucophores were counted again. For temperature-shift experiments using the *kita*^{j1e99} allele, fish were reared at permissive temperature (25 °C), intermediate temperature (28 °C), or restrictive temperature (33 °C) until melanophores and melanoleucophores of controls at permissive temperature had populated the distal dorsal fin (9.2 SSL) (20, 27).

TEM
Fin portions were amputated and prefixed in 1:1 4% glutaraldehyde and PBS at room temperature for 30 minutes to maintain structure. Fins were then fixed in sodium cacodylate buffered 4% glutaraldehyde overnight at 4°C. Tissue was post-fixed in 2% osmium tetroxide, block stained in 1% uranyl acetate overnight at 4°C, then dehydrated with an ethanol series. Tissue was then infiltrated with a 1:1 propylene oxide:Durcupan resin for 2 hours followed by fresh Durcupan resin overnight and flat embedded prior to polymerization. Blocks were thin sectioned on a Leica EM UC7 and sections images on a JEOL 1230 transmission electron microscope. Identity of pigment-containing organelles was inferred by comparison to published observations of melanosomes, iridophore reflecting platelets, xanthophore and erythrophore pterinosomes and carotenoid vesicles, and organelles of leucophores and leucophore-like cells [e.g., (13, 17, 28-36)].

Hyperspectral Imaging
Amputated fins were placed in PBS at room temperature and spectral measurements were performed using a PARISS hyperspectral imaging system (Lightform, Inc.), which acquires 380–980 nm spectra instantaneously from each pixel (1.25 µm x 1.25 µm) in a line of pixels. The microscope stage was then set to move adjacently to acquire another line of pixels. The

PARISS software stitches these lines of pixels together to make a grayscale 2D image (reflecting the intensity of spectra) which was used to choose the spatial location of the spectra of interest. The hyperspectral imager was mounted on a Nikon Eclipse 80i microscope. Spectral calibration was performed using a MIDL Hg^{+}/Ar^{+} wavelength calibration lamp (Lightform Inc.) with accuracy better than 2 nm. Cells spectra were acquired under both specular reflectance and transmittance mode, using a tungsten halogen light source with a Nikon NCB11 filter, and a 20x 0.50 NA objective. Reflectance spectra were normalized using a standard silver mirror (Thorlabs, Inc.). All spectra were smoothed with a moving average of 3 as conventionally performed, and plotted using Matlab.

Pteridine Autofluorescence

To assess pteridine content of leucophores, amputated fins were imaged before and after exposure to dilute ammonia (pH 10.0), which liberates pteridines from protein carriers resulting in autofluorescence under DAPI illumination (3, 4).

Mass Spectrometry

Each of three fin regions were excised from adult fish that were either wild-type, or mutant for *mitfa* or *ltk* (*n*=20 per genotype): (i) dorsal fin, distal region containing melanoleucophore stripe, including xanthophores as well; (ii) dorsal fin, adjacent to melanoleucophore stripe, containing only melanophores and xanthophores, and of size equivalent to i; (iii) anal fin, proximal light "interstripes" containing xantholeucophores and iridophores, as well as intervening dark stripe of melanophores. Purines were extracted from fin tissue in 50 µl 1M NaOH at 37 °C. Liquid chromatography/mass spectrometry (LCMS) was performed using an Agilent 1100 HPLC system equipped with a Waters XTerra MS C18, 5 µm, 4.6 Å 50 mm column or Poroshell 120 EC-C18 4.6 Å x 100 mm column. An Agilent photodiode array detector and an in-line Agilent 6130 single quadrupole mass spectrometer were used for detection. The analytical HPLC method used gradient elution from 0% to 95% acetonitrile in water (0.1% formic acid) over 6 min and Agilent ChemStation software were used for quantification. Chromatograms of the compounds were monitored at 254 nm, 210 nm, and 280 nm.

Raman Spectroscopy

Fin portions were amputated and placed in PBS. Guanine references were prepared by recrystallizing guanine powder (Sigma Aldrich, G6779) (37). Samples were prepared by sandwiching prepared tissues or crystals between quartz coverslips (Ted Pella, Inc., Cat. No. 26016) and glass microscope slides (VWR, Cat. No. 16004-422). All data were collected at RT using a custom-built Raman microscope (38). Briefly, the 514-nm line of an argon-ion laser (CVI Melles Griot, 35-MAP-431-200) was passed through a clean-up filter (Semrock, LL01-514-25) and then directed into a modified inverted microscope (Olympus IX71). Excitation light (~30 mW at the sample) was directed to the sample using a dichroic mirror (Semrock, LPD01-514RU-25x36-1.1) and a 60x long-working distance objective (Olympus, LUCPlanFL N 60X/0.70). Spontaneous Raman Stokes scattering was collected through the same objective, filtered (Semrock, LP02-514RE-25) to remove any residual excitation light or Rayleigh scattering, and then directed into a 320 mm focal length (f/4.1 aperture) imaging spectrometer (Horiba Scientific, iHR 320) first through a 400 µm pinhole (Thorlabs) and a 50 µm slit, and dispersed using a 1200 g/mm grating. Individual spectra were collected for 5–7 s acquisitions (x25–30) from 500–3700 cm^{-1} with high gain enabled on a liquid nitrogen cooled, back illuminated deep-depletion CCD array (Horiba Scientific, Symphony II, 1024 × 256 px, 26.6 mm × 6.6 mm, 1 MHz repetition rate). Bright field images were collected using a USB 2.0 camera (iDS, UI-1220-C). Daily calibration of imaging spectrometer was done using neat cyclohexane (20 µL in a sealed

capillary tube). Bandpass and accuracy were found to be <12 cm^{-1} and ±1 cm^{-1}, respectively. All Raman spectra were corrected by applying a baseline polynomial fit (Lab Spec 6 software).

Isolation of Cells for Single Cell RNA-Sequencing

Fins were amputated from fish expressing both *pnp4a:palmmCherry* and *tyrp1b:palmmCherry*. To approximately normalize capture of relevant cell types by quantity and improve the likelihood of recovering cells at intermediate states of differentiation, we extracted distal dorsal fin regions (~10 mm standard length, SL; *n*=20) and proximal interstripe anal fin regions (~14 mm SL; *n*=10). Tissue was enzymatically dissociated with Liberase (0.25 mg/ml in dPBS) at 25°C for 15 min followed by manual trituration with a flame polished glass pipette for 5 min. Cell suspensions were then filtered through a 70 µm Nylon cell strainer to obtain a single cell suspension. Liberated cells were re-suspended in 1% BSA / 5% FBS in dPBS and DAPI (0.1 µg/ml 15 min) before FACS purification. All plastic and glass surfaces of cell contact were coated with 1% BSA in dPBS before to use. Prior to sorting for fluorescence levels, single cells were isolated by sequentially gating cells according to their SSC-A vs. FSC-A, FSC-H vs FSC-W and SSC-H vs SSC-W profiles according to standard flow cytometry practices. Cells with high levels of DAPI staining were excluded as dead or damaged. Cells from wild-type zebrafish were used as negative control to determine gates for detection of mCherry and GFP fluorescence, and then cells from transgenic fish were purified according to these gates. All samples were kept on ice, except during Liberase incubation, and then sorted chilled.

Single Cell Collection, Library Construction and Sequencing

Following FACS, cells were pelleted and resuspended in 0.04% ultrapure BSA (ThermoFisher Scientific). We targeted 4000 cells for capture in a single lane using the Chromium platform (10X Genomics). Single-cell mRNA libraries were prepared using the single-cell 3' solution V2 kit (10X Genomics). Quality control and quantification assays were performed using a Qubit fluorometer (ThermoFisher) and a D1000 Screentape Assay (Agilent). Libraries were sequenced on an Illumina NextSeq 500 using 75-cycle, high output kits (read 1: 26 cycles, i7 Index: 8 cycles, read 2: 57 cycles). The full library was sequenced to an average depth of ~130 million reads. This resulted in an average read depth of 28,000 reads/cell.

scRNA-Seq Data Processing

We built a zebrafish STAR genome index using gene annotations from Ensembl GRCz10 plus manually annotated entries for mCherry transcript, filtered for protein-coding genes (with Cell Ranger *mkgtf* and *mkref* options). Final cellular barcodes and Unique Molecular Identifiers (UMIs) were determined using Cell Ranger 2.0.2 (10X Genomics) and cells were filtered to include only high-quality cells. Cell Ranger defaults for selecting cell-associated barcodes versus barcodes associated with empty partitions were used, resulting in a final gene-barcode matrix containing 4,594 barcoded cells and gene expression counts. scRNA-Seq dataset was deposited in the NCBI GEO database (accession #GSE130526).

UMAP Visualization and Clustering

We used Uniform Manifold Approximation and Projection (UMAP) to project multidimensional transcriptomic cell space (39) in two dimensions and performed Louvain clustering (40) using the reduceDimension and clusterCells functions in Monocle (v.2.99.1) using default parameters (except for, reduceDimension: reduction_method=UMAP, metric=cosine, n_neighbors=20, mid_dist=0.4; clusterCells: res=1e-3, k=25). We assigned clusters to cell types based on comparison of genes detected (Dataset S1) to published cell-type specific markers. All genes were given as input to Principal Components Analysis (PCA). The top 30 principal components (high-loading, based on the associated scree plot) were then used as input to UMAP for

generating either 2D projections of the data. For subclustering of pigment cell clusters (melanophores, melanoleucophores, xanthophores, and xantholeucophores) we re-subsetted the data and applied UMAP dimensionality reduction and Louvain clustering.

Differential Expression Analysis to Determine Cell-type Markers

To identify cell-type specific genes, we used the principalGraphTest function in Monocle3 (v.2.99.1) with default parameters (41). This function uses a spatial correlation analysis, the Moran's I test, to assess spatially restricted gene expression patterns in low dimensional space. We selected markers by optimizing for high specificity, expression levels and effect sizes within clusters (Dataset S2). Expression levels presented are normalized by size factor (ratio of total UMI counts for each cell and geometric mean of total UMI from all cells) (41).

Pigment Cell Subcluster Assignment and Verification

Pigment cell subclusters were broadly assigned as either xanthophores and xantholeucophores or melanophores and melanoleucophores based on *aox5* or *tyrp1b* expression (*SI Appendix* Fig. S6*F*). To further distinguish among these cell types we used RT-PCR to assay the top marker identified by scRNA-Seq for each cell type by specificity and expression (Dataset S2). Distal dorsal fin tissue containing melanoleucophores, melanophores and xanthophores, or tissue from the proximal two interstripe regions of the anal fin, containing xantholeucophores, was dissociated (see above) and 100 cells of each type collected by mouth-pipette using a needle that had been coated in sterile 5% FBS / 1% BSA overnight at 4 °C. Cells were identified by phenotype under incident light and washed (expelled and recollected) 3 times in dPBS before final collection in lysis buffer for mRNA capture. mRNA was collected using the Ambion RNAqueous-Micro kit and cDNA was synthesized using oligo-dT primed SuperScript IV reverse transcriptase. Primers were designed to have at least one sequence that overlapped and exon/intron boundary. PCR using Q5 High-Fidelity DNA Polymerase ran for 30 cycles at 98 °C—10 sec, 60 °C—20 sec, 72 °C—30 sec and amplicons were separated on a 1% agarose gel. Primers were: *entpd3*(f)-CTTATGTTTCCCGTGGACTAAAGTA, *entpd3*(r)-ATTGGATCTCCCTTCATTTGTCATA; *ocaa2*(f)-TATTGTCGTTCTGTGTTCACTGTTT, *ocaa2*(r)-ATTATACAGCACCTGCTGAGTTCTT; *sfrp1a*(f)-GTGAGTTTGCCATTAAGACCAAGAT, *sfrp1a*(r)-GAGAAGGTACTGTTTGTCCACCTT; *scinla*(f)-GGTAATGAGTGTTCTCAGGATGAAA, *scinla*(r)-ATTGATAGATGTCCTTGCCAAGAT.

Trajectory Analysis

The top 100 highly dispersed genes within melanophore and melanoleucophore clusters were chosen as feature genes to resolve pseudotemporal trajectories using the setOrderingFilter, reduceDimension, and orderCells functions in Monocle (v2.9.0) using default parameters with the exception of setting max_components = 2 and num_dim = 20 to generate the trajectory in 2D with the top 20 PCs (high-loading based on scree plot) during dimensionality reduction.

Development and Analysis of Pathway Signature Scores

Gene sets for signature scores for purine synthesis (42), melanin synthesis (43) pteridine synthesis (3) and carotenoid deposition (44) were manually curated from the literature and ZFIN (45). Signature scores were calculated by generating z-scores [using scale()] of the mean of expression values (log transformed, size factor normalized) from genes in a given set.

Physiological Response Testing

To evaluate physiological response during background adaptation to light or dark backgrounds individual fish (total n=6; n=3 per replicate with two replicates per background) were adapted in a 500 mL black (dark background) or white (light background) colored beaker under constant

light for 5 minutes. Fish were then anesthetized with MS222 in the test beaker and cells from a central inter-ray region of the distal dorsal fin (melanophores and melanoleucophores) or of the anal fin second interstripe (proximal-distal; xantholeucophores) were scored under incident light. Cells were scored as either contracted or dispersed according to stages 1–3 or 4–5, respectively, of the Hogben and Slome scale (46).

Behavioral Assays

***Testing Arena*:** To test for a behavioral response to the presence of melanoleucophores, wild-type NHGR1 strain *D. rerio* were chosen for the uniformity of their pigment cell complements and limited allelic variation (47). Fish were subjected to assays consisting of three location options: open water (i.e., center third of tank), or proximity to conspecifics on either end of the tank (left or right thirds). The tank (30 cm long, 14 cm wide x 18 cm tall) was divided into three chambers with Plexiglass transparent to UV light: a test chamber in the central portion of the tank (18 cm long x 14 cm wide x 18 cm tall) and two chambers for stimulus shoals on either side (each 6 cm long x 14 cm wide x 18 cm tall). For testing, chambers were filled with system water to a depth of 14 cm. Full spectrum LED lights (Draco Broadcast Dracast LED500, 5600K) were positioned 1 m above the tank to allow even lighting (~5500 lux) across the entire test arena. To avoid disturbance, the tank was placed in an open-top black box 52 cm long x 40 cm wide x 48 cm tall) with a hole 24 cm long x 22 cm tall) for a video camera cut in one side. Black plastic was draped around the camera to prevent fish from viewing the environment beyond the assay arena. All fish were recorded at 30 frames per sec with a Panasonic HC-V770 digital camera.

***First Approach and Shoaling Assays*:** Stimulus shoals comprising two fish of the same sex were placed into the tank using a fish net and acclimated in the shoal chambers for 10 min prior to the onset of each testing round. Each testing round consisted of four test fish (10 min per fish; 40 min total). Test fish were dropped into the acclimation chamber (opaque cylinder, 4 cm inner diameter) using a fish net. After 5 min of acclimation, test fish were released into the test chamber for 5 min. After assaying the behavior of each test fish and after a complete round of testing, test fish and shoal fish were removed from the tank using a fish net. Between each testing round, the tank was rinsed with 65 °C water for 10 min followed by a brief rinse with fish system water before all chambers of the tank were refilled with system water. To control for possible circadian effects on sensory perception, motivation, or locomotion, all fish were assayed between 8 and 12 h after lights-on (13:00 and 17:00).

In preliminary assays, the suitability of the testing arena was confirmed by verifying that test fish would preferentially shoal with other fish as expected (48, 49), when presented with compartments either containing fish or not containing fish (*SI Appendix* Fig. S8*A*). Preference towards fish or empty chamber was tested with a reciprocal design. Male test fish (n=15 total) were tested with either a male (n=8 tests) or female (n=7 tests) shoal. Likewise, female test fish (n=14) were tested with either a male (n=7 tests) or female (n=7 tests) shoal. Numbers of melanoleucophores per fish did not differ significantly between sexes ($F_{1,10}$=0.1, P=0.8). Placement of the shoal was randomized for each round of testing. Test fish were scored for total times spent in each of three segments of the test chamber: the 6 cm closest to the stimulus shoal, the 6 cm closest to the empty compartment, or the 6 cm in the central portion of the test chamber. For quantifying the preference of test fish to shoal in the vicinity of stimulus fish vs. an empty compartment, we calculated seconds spent swimming within 6 cm of the stimulus shoal – seconds spent swimming within 6 cm of the empty stimulus compartment; under a null hypothesis of no preference the mean for this value should be 0 sec.

To test for individual abilities to detect and respond to melanoleucophores, fish either had tissue containing melanoleucophores excised (ML–) or had melanoleucophore-containing tissue left intact (sham-manipulated, ML+). Each ML– fish had a thin strip of melanoleucophore-

containing tissue removed from the distal edge of the dorsal fin and the distal tips of the caudal fin with microdissection scissors and fine forceps (*SI Appendix* Fig. S8*B*). ML+ fish were lesioned with single inward cuts to the dorsal fin, without tissue removal, at anterior and posterior edges. To control for effects of tissue removal in general, ML+ fish also had tissue excised from the central portion of the caudal fin, between the dorsal and ventral lobes, and along the caudal most edge of the anal fin. ML– fish were correspondingly lesioned with a single inward cut on the rostral edge of the area removed from the anal fin of sham-manipulated fish. Conceptually similar experiments have been used to test features of fins in other contexts and with other species (50-53). Prior to testing, all fish were allowed to recover and partially regenerate lost tissue, though not melanoleucophores, for 2 d in home tanks. ML– were housed with other ML– fish whereas ML+ fish were housed with other ML+ fish, with adjacent tanks alternating between lesion type so that all fish were in visual proximity to both ML– and ML+ fish. Because stimulus shoals might respond differently to test fish with or without melanoleucophores, and such effects might influence test fish responses, both test fish and stimulus fish were assigned randomly to melanoleucophore-excised or sham-manipulated groups. Preliminary analyses did not reveal gross alterations in swimming behavior resulting from melanoleucophore-excision or sham-manipulation. Likewise, no significant effects on test fish behavior were observed depending on whether test fish themselves were melanoleucophore-excised or sham-manipulated ($P>0.5$); this factor was removed from subsequent analyses.

For testing effects of melanoleucophore complement on behavior, male test fish ($n=16$) were presented with two shoals of the same sex, one of which was ML– and one of which was ML+ (male stimulus shoals, $n=9$ tests; female stimulus shoals, $n=7$ tests). Female test fish ($n=18$) were likewise presented with same sex ML– or ML+ same-sex shoals (male stimulus shoals, $n=8$ tests; female stimulus shoals, $n=10$ tests). Placement side of ML– vs. ML+ stimulus shoals was randomized for each round of testing. Test fish were assayed for total time shoaling in proximity to ML– vs. ML+ stimulus fish according to time accumulated in each third of the test chamber closest to one shoal or the other. Test fish were also assayed to determine whether ML– or ML+ fish were first approached upon release into the test chamber.

***Behavior Quantification*:** Videos of fish were scored using Tracker Video Analysis and Modeling Tool software (version 5.0.5; https://physlets.org/tracker). Frames per step was set to 30 to determine test fish position every 1 sec. Fish positions were assessed for the entire duration of the shoaling test (i.e., 5 min or 300 steps) using the Point Mass feature with mass set to the default (1.0 kg). The coordinate system was established with the point of origin at the shoal (fish vs. no fish assay) or the ML– fish (melanoleucophore response assay). Parameters quantified included x position and y position. The test arena was divided evenly into three domains along the x-axis. The position of first approach was defined as the closest x position of the first approach within either of the two domains closest to the shoal chambers.

Statistical analysis

Analyses were performed using JMP 14.0 for Macintosh (SAS Institute, Cary NC) or *R* [version 3.5.0] (54)

References

1. McCluskey BM & Postlethwait JH (2015) Phylogeny of Zebrafish, a "Model Species," within Danio, a "Model Genus". *Mol Biol Evol* 32(3):635-652.
2. Parichy DM (2015) Advancing biology through a deeper understanding of zebrafish ecology and evolution. *Elife* 4.
3. Ziegler I (2003) The pteridine pathway in zebrafish: regulation and specification during the determination of neural crest cell-fate. *Pigment Cell Res* 16(3):172-182.
4. Odenthal J*, et al.* (1996) Mutations affecting xanthophore pigmentation in the zebrafish, Danio rerio. *Development* 123:391-398.
5. Saunders LM*, et al.* (2019) Thyroid hormone regulates distinct paths to maturation in pigment cell lineages. *eLife* In revision.
6. Toomey MB*, et al.* (2017) High-density lipoprotein receptor SCARB1 is required for carotenoid coloration in birds. *Proc Natl Acad Sci U S A* 114(20):5219-5224.
7. Parichy DM, Elizondo MR, Mills MG, Gordon TN, & Engeszer RE (2009) Normal table of postembryonic zebrafish development: staging by externally visible anatomy of the living fish. *Dev Dyn* 238(12):2975-3015.
8. Parichy DM, Ransom DG, Paw B, Zon LI, & Johnson SL (2000) An orthologue of the *kit*-related gene *fms* is required for development of neural crest-derived xanthophores and a subpopulation of adult melanocytes in the zebrafish, *Danio rerio*. *Development* 127(14):3031-3044.
9. Parichy DM, Rawls JF, Pratt SJ, Whitfield TT, & Johnson SL (1999) Zebrafish sparse corresponds to an orthologue of c-kit and is required for the morphogenesis of a subpopulation of melanocytes, but is not essential for hematopoiesis or primordial germ cell development. *Development* 126(15):3425-3436.
10. Lopes SS*, et al.* (2008) Leukocyte tyrosine kinase functions in pigment cell development. *PLoS Genet* 4(3):e1000026.
11. Lister JA, Robertson CP, Lepage T, Johnson SL, & Raible DW (1999) nacre encodes a zebrafish microphthalmia-related protein that regulates neural-crest-derived pigment cell fate. *Development* 126(17):3757-3767.
12. Rawls JF & Johnson SL (2000) Zebrafish kit mutation reveals primary and secondary regulation of melanocyte development during fin stripe regeneration. *Development* 127(17):3715-3724.
13. Hama T (1975) Chromatophores and iridocytes. *Medaka (Killifish) Biology and Strains*, ed Yamamoto T (Keigaku Publishing Co., Tokyo, Japan), pp 138–153.
14. Ilicic T*, et al.* (2016) Classification of low quality cells from single-cell RNA-seq data. *Genome Biol* 17:29.
15. Tu S & Johnson SL (2011) Fate restriction in the growing and regenerating zebrafish fin. *Dev Cell* 20(5):725-732.
16. Tu S & Johnson SL (2010) Clonal analyses reveal roles of organ founding stem cells, melanocyte stem cells and melanoblasts in establishment, growth and regeneration of the adult zebrafish fin. *Development* 137(23):3931-3939.
17. Salis P*, et al.* (2019) Developmental and comparative transcriptomic identification of iridophore contribution to white barring in clownfish. *Pigment Cell Melanoma Res*.
18. Eom DS, Bain EJ, Patterson LB, Grout ME, & Parichy DM (2015) Long-distance communication by specialized cellular projections during pigment pattern development and evolution. *Elife* 4.
19. McMenamin SK*, et al.* (2014) Thyroid hormone-dependent adult pigment cell lineage and pattern in zebrafish. *Science* 345(6202):1358-1361.
20. Rawls JF & Johnson SL (2001) Requirements for the kit receptor tyrosine kinase during regeneration of zebrafish fin melanocytes. *Development* 128(11):1943-1949.
21. Johnson SL, Nguyen AN, & Lister JA (2011) mitfa is required at multiple stages of melanocyte differentiation but not to establish the melanocyte stem cell. *Dev Biol* 350(2):405-413.
22. Dooley CM*, et al.* (2013) Slc45a2 and V-ATPase are regulators of melanosomal pH homeostasis in zebrafish, providing a mechanism for human pigment evolution and disease. *Pigm Cell Melanoma R* 26(2).
23. Shah AN, Davey CF, Whitebirch AC, Miller AC, & Moens CB (2016) Rapid Reverse Genetic Screening Using CRISPR in Zebrafish. *Zebrafish* 13(2):152-153.

24. Kawakami K*, et al.* (2004) A transposon-mediated gene trap approach identifies developmentally regulated genes in zebrafish. *Dev Cell* 7(1):133-144.
25. Kwan KM*, et al.* (2007) The Tol2kit: a multisite gateway-based construction kit for Tol2 transposon transgenesis constructs. *Dev Dyn* 236(11):3088-3099.
26. Spiewak JE*, et al.* (2018) Evolution of Endothelin signaling and diversification of adult pigment pattern in Danio fishes. *PLoS Genet* 14(9):e1007538.
27. Hultman KA, Bahary N, Zon LI, & Johnson SL (2007) Gene Duplication of the zebrafish kit ligand and partitioning of melanocyte development functions to kit ligand a. *PLoS Genet* 3(1):e17.
28. Hirata M, Nakamura K, & Kondo S (2005) Pigment cell distributions in different tissues of the zebrafish, with special reference to the striped pigment pattern. *Dev Dyn* 234(2):293-300.
29. Hirata M, Nakamura K, Kanemaru T, Shibata Y, & Kondo S (2003) Pigment cell organization in the hypodermis of zebrafish. *Dev Dyn* 227(4):497-503.
30. Granneman JG*, et al.* (2017) Lipid droplet biology and evolution illuminated by the characterization of a novel perilipin in teleost fish. *eLife* 6.
31. Djurdjevic I, Kreft ME, & Susnik Bajec S (2015) Comparison of pigment cell ultrastructure and organisation in the dermis of marble trout and brown trout, and first description of erythrophore ultrastructure in salmonids. *J Anat* 227(5):583-595.
32. Kottler VA*, et al.* (2014) Multiple pigment cell types contribute to the black, blue, and orange ornaments of male guppies (Poecilia reticulata). *PLoS One* 9(1):e85647.
33. Bagnara JT (1983) Developmental aspects of vertebrate chromatophores. *Amer. Zool.* 23:465–478.
34. Fujii R (1993) Cytophysiology of fish chromatophores. *Int Rev Cytol* 143:191–255.
35. Schartl M*, et al.* (2016) What is a vertebrate pigment cell? *Pigment Cell Melanoma Res* 29(1):8-14.
36. Takeuchi IK (1976) Electron microscopy of two types of reflecting chromatophores (iridophores and leucophores) in the guppy, Lebistes reticulatus Peters. *Cell Tissue Res* 173(1):17-27.
37. Gur D*, et al.* (2015) Structural Basis for the Brilliant Colors of the Sapphirinid Copepods. *J Am Chem Soc* 137(26):8408-8411.
38. Flynn JD & Lee JC (2018) Raman fingerprints of amyloid structures. *Chem Commun (Camb)* 54(51):6983-6986.
39. Becht E*, et al.* (2018) Dimensionality reduction for visualizing single-cell data using UMAP. *Nat Biotechnol*.
40. Vincent D. Blondel J-LG, Renaud Lambiotte, Etienne Lefebvre (2008) Fast Unfolding of Communities in Large Networks. *ArXiv e-prints* 0803.0476.
41. Qiu X*, et al.* (2017) Single-cell mRNA quantification and differential analysis with Census. *Nat Methods* 14(3):309-315.
42. Ng A, Uribe RA, Yieh L, Nuckels R, & Gross JM (2009) Zebrafish mutations in gart and paics identify crucial roles for de novo purine synthesis in vertebrate pigmentation and ocular development. *Development* 136(15):2601-2611.
43. Braasch I, Schartl M, & Volff JN (2007) Evolution of pigment synthesis pathways by gene and genome duplication in fish. *BMC Evol Biol* 7:74.
44. Toews DPL, Hofmeister NR, & Taylor SA (2017) The Evolution and Genetics of Carotenoid Processing in Animals. *Trends Genet* 33(3):171-182.
45. Ruzicka L*, et al.* (2015) ZFIN, The zebrafish model organism database: Updates and new directions. *Genesis* 53(8):498-509.
46. Fingerman M (1963) *The Control of Chromatophores* (Macmillan Company, New York) p 184.
47. LaFave MC, Varshney GK, Vemulapalli M, Mullikin JC, & Burgess SM (2014) A Defined Zebrafish Line for High-Throughput Genetics and Genomics: NHGRI-1. *Genetics* 198(1):167-170.
48. Engeszer RE, Ryan MJ, & Parichy DM (2004) Learned social preference in zebrafish. *Curr Biol* 14(10):881-884.
49. Engeszer RE, Wang G, Ryan MJ, & Parichy DM (2008) Sex-specific perceptual spaces for a vertebrate basal social aggregative behavior. *Proc Natl Acad Sci U S A* 105(3):929-933.
50. Keenleyside HHA (1955) Some aspects of the schooling behavior of fish. *Behaviour* 8:183–248.
51. Bischoff RL, Gould JL, & Rubenstein DI (1985) Tail size and female choice in the guppy (Poecilia reticulata). *Behav Ecol Sociobiol* 17:253–255.

52. Rowland WJ (1999) Studying Visual Cues in Fish Behavior: A Review of Ethological Techniques. *Environmental Biology of Fishes* 56(3):285-305.
53. Kang J, Nachtrab G, & Poss KD (2013) Local Dkk1 crosstalk from breeding ornaments impedes regeneration of injured male zebrafish fins. *Dev Cell* 27(1):19-31.
54. Team RC (2014) R: A language and environment for statistical computing. *R Foundation for Statistical Computing*.